The Heteronuclear Cluster Chemistry of the Group 1B Metals. Part 2.[1] Synthesis, *X*-Ray Crystal Structures, and Dynamic Behaviour of the Bimetallic Hexanuclear Group 1B Metal Cluster Compounds $[M_2Ru_4H_2(CO)_{12}(PPh_3)_2]$ (M = Cu, Ag, or Au)*

Mark J. Freeman and A. Guy Orpen
Department of Inorganic Chemistry, University of Bristol, Bristol BS8 1TS
Ian D. Salter
Department of Chemistry, University of Exeter, Exeter EX4 4QD

Treatment of dichloromethane solutions of the salt $[N(PPh_3)_2]_2[Ru_4(\mu\text{-}H)_2(CO)_{12}]$ with two equivalents of the complex $[M(NCMe)_4]PF_6$ (M = Cu or Ag) at −30 °C, followed by the addition of two equivalents of PPh_3, affords the mixed-metal cluster compounds $[M_2Ru_4(\mu_3\text{-}H)_2(CO)_{12}(PPh_3)_2]$ [M = Cu (**1**) or Ag(**2**)] in *ca.* 75% yield. The analogous gold species $[Au_2Ru_4(\mu_3\text{-}H)(\mu\text{-}H)(CO)_{12}(PPh_3)_2]$ (**5**) (*ca.* 60% yield) and reduced yields (*ca.* 50%) of (**1**) and (**2**) can be obtained by treating acetone solutions of the salt $[N(PPh_3)_2]_2[Ru_4(\mu\text{-}H)_2(CO)_{12}]$ with a dichloromethane solution containing two equivalents of the appropriate complex $[MX(PPh_3)]$ (M = Cu or Au, X = Cl; M = Ag, X = I), in the presence of $TlPF_6$. Single-crystal *X*-ray diffraction studies on each member of this series of Group 1B metal congeners show that all three clusters adopt the same metal core structure. Each metal skeleton consists of a tetrahedron of ruthenium atoms capped by a $M(PPh_3)$ (M = Cu, Ag, or Au) moiety, with one of the MRu_2 faces of the MRu_3 tetrahedron so formed further capped by a second $M(PPh_3)$ fragment to give a capped trigonal bipyramidal metal core geometry. For (**1**) and (**2**), the other two faces of the MRu_3 tetrahedron are each capped by triply bridging hydrido ligands but, in the case of (**5**), one of these hydrido ligands bridges a ruthenium–ruthenium edge only. In all three clusters, each ruthenium atom is ligated by three terminal carbonyl groups. Variable-temperature n.m.r. studies show that, at ambient temperature in solution, the coinage metals in all three clusters are exchanging between the two distinct sites in the capped trigonal bipyramidal metal cores, the CO ligands all exhibit dynamic behaviour involving complete intramolecular site exchange and, in addition, the PPh_3 groups of (**2**) are undergoing intermolecular exchange between clusters.

Over the last five years, there have been numerous reports[1–5] of mixed-metal cluster compounds in which one or more $Au(PR_3)$ (R = alkyl or aryl) moieties are incorporated into structures containing other different transition metals ligated by carbonyl groups. However, analogous species containing $M(PR_3)$ (M = Cu or Ag) fragment(s) have received much less attention.[1,6,7] In the first paper of this series,[1] we described our interest in conducting more detailed investigations into the chemistry of this type of copper and silver cluster and in experimentally comparing the bonding capabilities of $M(PR_3)$ (M = Cu, Ag, or Au) units by synthesizing series of analogous heteronuclear clusters containing one or more of these moieties. Herein we report the preparation of a series of bimetallic hexanuclear mixed-metal clusters containing two $M(PPh_3)$ groups and we discuss the similarities and differences in the structures and dynamic behaviour of the three Group 1B metal congeners.

While our work was in progress, Bruce and Nicholson[8] also obtained the gold–ruthenium cluster (**5**) (3% yield). However, these workers did not establish the structure of (**5**) by single-crystal *X*-ray diffraction analysis and, as they performed no n.m.r. spectroscopic studies on the cluster, they also failed to observe its dynamic behaviour. Preliminary accounts describing some of our results have already been published.[6,7]

Results and Discussion

Treatment of a dichloromethane solution of the salt $[N(PPh_3)_2]_2[Ru_4(\mu\text{-}H)_2(CO)_{12}]$[9] with two equivalents of the complex $[M(NCMe)_4]PF_6$ (M = Cu or Ag) at −30 °C

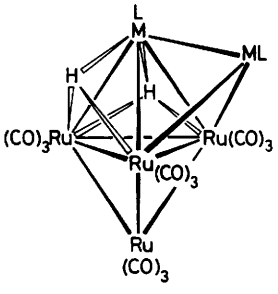

	M	L
(1)	Cu	PPh_3
(2)	Ag	PPh_3
(3)	Cu	NCMe
(4)	Ag	NCMe

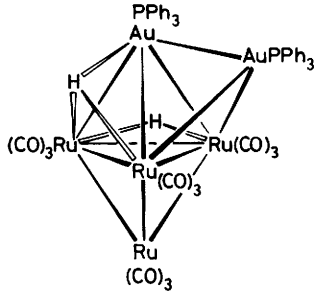

(5)

* 2,2,2,3,3,3,4,4,4,5,5,5-Dodecacarbonyl-1,2,3;1,2,4-di-μ_3-hydrido-1-triphenylphosphine-1,3,4-μ_3-(triphenylphosphinecuprio)-*cyclo*-coppertetraruthenium, 2,2,2,3,3,3,4,4,4,5,5,5-dodecacarbonyl-1,2,3;1,2,4-di-μ_3-hydrido-1-triphenylphosphine-1,3,4-μ_3-(triphenylphosphine-argentio)-*cyclo*-silvertetraruthenium, and 2,2,2,3,3,3,4,4,4,5,5,5-dodecacarbonyl-2,4-μ-hydrido-1,2,3-μ_3-hydrido-1-triphenylphosphine-1,3,4-μ_3-(triphenylphosphineaurio)-*cyclo*-goldtetraruthenium, respectively.

Supplementary data available: see Instructions for Authors, *J. Chem. Soc., Dalton Trans.*, 1987, Issue 1, pp. xvii—xx.

Table 1. Analytical[a] and physical data for the Group 1B metal heteronuclear cluster compounds

Compound	M.p. (decomp.)/°C	$\nu_{max.}$(CO)[b]/cm^{-1}	Yield (%)[c]	Analysis[d] C	H
(1) $[Cu_2Ru_4(\mu_3\text{-}H)_2(CO)_{12}(PPh_3)_2]$	123—126	2 071s, 2 032vs, 2 021vs, 2 005s, 1 988w, 1 974m, 1 938w br	76	41.5 (41.3)	2.2 (2.3)
(2) $[Ag_2Ru_4(\mu_3\text{-}H)_2(CO)_{12}(PPh_3)_2]$	167—170	2 069s, 2 030vs, 2 018vs, 2 002s, 1 981w, 1 969m, 1 936w br	74	39.3 (38.9)	2.5 (2.2)
(3) $[Cu_2Ru_4(\mu_3\text{-}H)_2(CO)_{12}(NCMe)_2]$[e]	—	2 072m, 2 034(sh), 2 022vs, 2 008(sh), 1 973m br, 1 945w br	—	—	—
(5) $[Au_2Ru_4(\mu_3\text{-}H)(\mu\text{-}H)(CO)_{12}(PPh_3)_2]$	143—147	2 070s, 2 043m, 2 033s, 2 022vs, 2 006s, 1 988m, 1 975m, 1 956(sh), 1 914(sh)	61	35.1 (34.7)	2.1 (1.9)

[a] Calculated values given in parentheses. [b] Measured in dichloromethane solution. [c] Based on ruthenium reactant. When two alternative routes to the cluster exist, the best yield is quoted. [d] Although large crystals of (1), (2), and (5), grown slowly over a period of days so that they were suitable for *X*-ray diffraction studies, are dichloromethane solvates, when *microcrystals* of these clusters were grown quickly for analysis, no evidence of dichloromethane of crystallization was found. [e] Cluster is too unstable to isolate as a pure compound.

Table 2. Hydrogen-1, phosphorus-31, and carbon-13 n.m.r. data[a] for the Group 1B metal heteronuclear cluster compounds

Cluster	θ_c/°C	^{1}H data[b]	^{31}P-{^{1}H} data[c]	^{13}C-{^{1}H} data[d]
(1)	Ambient	−16.93 [t, 2 H, μ_3-H, J(PH) 5], 7.23—7.39 (m, 30 H, Ph)	4.3 (s br)	198.0 (CO), 134.2 [d, C^2(Ph), J(PC) 14], 131.2 [C^4(Ph)], 130.6 [d, C^1(Ph), J(PC) 39], 129.4 [d, C^3(Ph), J(PC) 9]
	−90	−17.20 [d, 2 H, J(PH) 12]	6.8 (s), −0.4 (s)	201.0 (2 CO), 199.5 (2 CO), 198.0 and 197.8 (s and sh, 5 CO), 196.4 (2 CO), 192.9 (1 CO)
(2)	Ambient	−17.14 [br t, 2 H, μ_3-H, J(AgH)$_{av}$ 12], 7.27—7.39 (m, 30 H, Ph)	*ca.* 23 (s vbr), *ca.* 10 (s vbr)	[e]198.5 (CO), 134.1 [d, C^2(Ph), J(PC) 17], 131.3 [C^4(Ph)], 129.6 [d, C^3(Ph), J(PC) 9]
	−90	−17.17 [d of d, 2 H, J(AgH)$_{av}$ 27, J(PH) 9]	18.4 [2 × d of d, ^1J(^{109}AgP) 565, ^1J(^{107}AgP) 490, ^2J(AgP)$_{av}$ 8], 13.4 [2 × d of d, ^1J(^{109}AgP) 473, ^1J(^{107}AgP) 410, ^2J(AgP)$_{av}$ 12]	201.7 (2 CO), 200.3 (2 CO), 199.0 and 198.8 (s and sh, 3 CO), 198.4 (2 CO), 196.2 (2 CO), 191.3 (1 CO)
	−50	−17.16 [t of t, 2 H, J(AgH)$_{av}$ 14, J(PH) 5]		
(5)	Ambient[f]	−14.67 [t, 2 H, μ_3-H, J(PH) 5], 7.21—7.55 (m, 30 H, Ph)	[f]58.7 (s)	[g]199.6 (CO), 134.2 [AA'X pattern, C^2(Ph), N(PC) 15], 131.7 [AA'X pattern, C^1(Ph), N(PC) 51], 131.4 [C^4(Ph)], 129.3 [AA'X pattern, C^3(Ph), N(PC) 12]
	−90	*ca.* −14 (s vbr, 2 H)	*ca.* 51 (s vbr)	*ca.* 201 (vbr), 199.2 (br)

[a] Chemical shifts (δ) in p.p.m., coupling constants in Hz. [b] Measured in [$^2H_2$]dichloromethane solution, unless otherwise stated. At −90 and −50 °C only the data for the hydrido ligand are presented. [c] Hydrogen-1 decoupled, measured in [$^2H_2$]dichloromethane solution unless otherwise stated, chemical shifts positive to high frequency of 85% H_3PO_4 (external). [d] Hydrogen-1 decoupled, measured in [$^2H_2$]dichloromethane–CH_2Cl_2 solution, chemical shifts positive to high frequency of $SiMe_4$, sh = shoulder. [e] Only one half of the doublet for C^1(Ph) is visible (δ 130.4 p.p.m.), the other half is obscured. [f] Measured in [$^2H_1$]chloroform solution. [g] N(PC) = |J(PC) + J(P'C)|.

incorporates two M(NCMe) units into the cluster dianion and the subsequent addition of two equivalents of PPh_3 affords the dark red cluster compounds $[M_2Ru_4(\mu_3\text{-}H)_2(CO)_{12}(PPh_3)_2]$ [M = Cu (**1**) or Ag (**2**)] in *ca.* 75% yield. The two intermediate species $[M_2Ru_4(\mu_3\text{-}H)_2(CO)_{12}(NCMe)_2]$ [M = Cu (**3**) or Ag (**4**)] are too unstable to be isolated as pure compounds, but the lability of their MeCN groups can be conveniently utilized for *in situ* ligand-exchange reactions.[7] The analogous gold cluster $[Au_2Ru_4(\mu_3\text{-}H)(\mu\text{-}H)(CO)_{12}(PPh_3)_2]$ (**5**) is readily obtained as a dark red crystalline compound, in *ca.* 60% yield, by treating an acetone solution of the salt $[N(PPh_3)_2]_2[Ru_4(\mu\text{-}H)_2(CO)_{12}]$ with a dichloromethane solution containing two equivalents of the complex $[AuCl(PPh_3)]$, in the presence of $TlPF_6$. The previously reported[5] dark green heptanuclear cluster, $[Au_3Ru_4(\mu_3\text{-}H)(CO)_{12}(PPh_3)_3]$, is also formed (6% yield) as a by-product of this preparation. Similar reactions in which the complexes $[MX(PPh_3)]$ (M = Cu, X = Cl; M = Ag, X = I) are utilized in place of $[AuCl(PPh_3)]$ afford reduced yields (*ca.* 50%) of (**1**) and (**2**).

The clusters (**1**), (**2**), and (**5**) were characterized by microanalyses and by spectroscopic measurements (Tables 1 and 2). The i.r. spectra of (**1**) and (**2**) are almost identical and they are also closely similar to that of (**5**), implying that all three Group 1B metal congeners share the same metal core geometry. The n.m.r. spectroscopic data and microanalyses are fully consistent with the proposed formulations for (**1**), (**2**), and (**5**), but to investigate the structures of this series of clusters in detail, single-crystal *X*-ray diffraction studies were performed on all three compounds. Discussion of the variable-temperature n.m.r. spectroscopic data is best deferred until the *X*-ray diffraction results have been described.

Crystals of (**1**) and (**2**), grown from dichloromethane–light petroleum mixtures, are essentially isomorphous dichloromethane solvates, differing only in details of bond lengths and angles, solvent disorder, and phenyl group orientation. The molecular structures of (**1**) and (**2**) are illustrated in Figure 1, which shows the crystallographic numbering scheme. The interatomic distances and bond angles are summarized in Tables 3 and 4. The *X*-ray diffraction study on crystals of (**5**), grown from dichloromethane–diethyl ether–light petroleum,

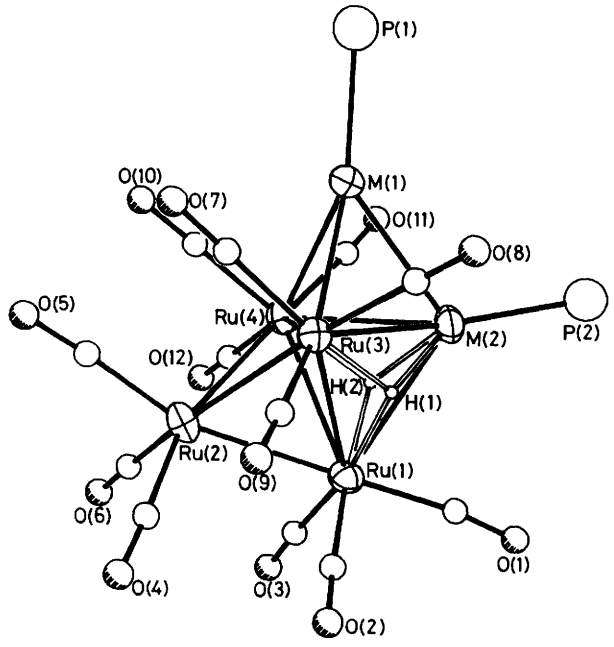

Figure 1. Molecular structure of $[M_2Ru_4(\mu_3\text{-}H)_2(CO)_{12}(PPh_3)_2]$ [M = Cu (**1**) or Ag (**2**)], showing the crystallographic numbering. Phenyl groups have been omitted for clarity and only the oxygen atom of each carbonyl ligand has been labelled; the carbon atom of each group has the same number as the oxygen atom

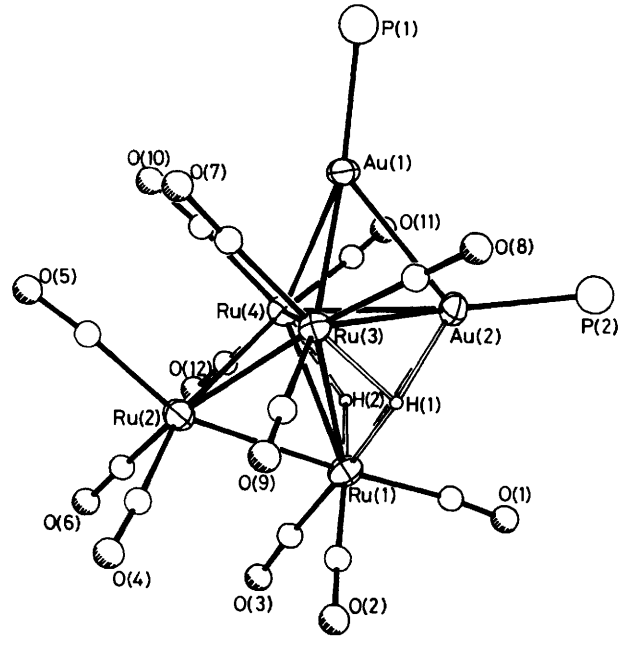

Figure 2. Molecular structure of $[Au_2Ru_4(\mu_3\text{-}H)(\mu\text{-}H)(CO)_{12}(PPh_3)_2]$ (**5**), showing the crystallographic numbering. Phenyl groups have been omitted for clarity and only the oxygen atom of each carbonyl ligand has been labelled; the carbon atom of each group has the same number as the oxygen atom

reveals that this cluster also crystallizes as a dichloromethane solvate and that its molecular structure is similar to those of (**1**) and (**2**), apart from the bonding mode of one hydrido ligand. The molecular structure of (**5**) is illustrated in Figure 2, which

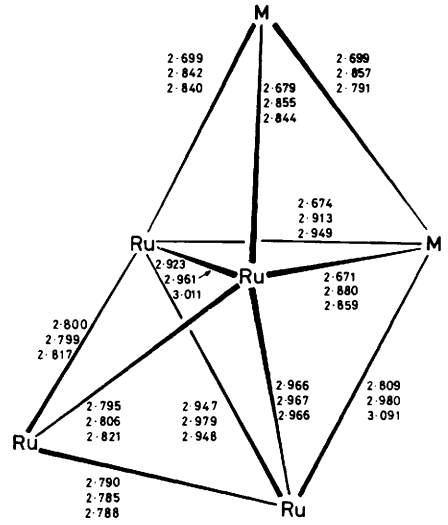

Figure 3. A comparison of the metal–metal separations (Å) within the capped trigonal bipyramidal metal cores of $[M_2Ru_4H_2(CO)_{12}(PPh_3)_2]$ [M = Cu (**1**) or Ag (**2**)], showing the crystallographic (**1**), then for (**2**), and finally for (**5**)

shows the crystallographic numbering scheme. The interatomic distances and bond angles are summarized in Table 5. All three of the clusters exhibit a capped trigonal bipyramidal metal core geometry, consisting of a tetrahedron of ruthenium atoms, with one face [Ru(1)Ru(3)Ru(4)] capped by a $M(PPh_3)$ (M = Cu, Ag, or Au) moiety [Group 1B metal site M(2)] and one of the faces [M(2)Ru(3)Ru(4)] of the MRu_3 tetrahedron so formed further capped by a second $M(PPh_3)$ fragment [Group 1B metal site M(1)]. Each ruthenium atom is ligated by three essentially terminal carbonyl ligands, which show little deviation from linearity. For (**1**) and (**2**), the potential energy minimization program HYDEX[10] and refinement of hydrogen positions against the *X*-ray data suggest that the two hydrido ligands adopt positions capping the M(2)Ru(1)Ru(3) and M(2)Ru(1)Ru(4) faces of the cluster. In the case of (**5**), the hydrido ligands were refined to much more asymmetrical positions with respect to Au(2) [Au(2)–H(1) 2.04(11), Au(2) · · · H(2) 2.76(11) Å, *cf.* Cu–H 1.62(5) in (**1**) and Ag–H 1.72(5) Å in (**2**)] suggesting that H(1) is triply bridging the Au(2)Ru(1)Ru(3) face of the cluster, whereas H(2) edge-bridges the Ru(1)–Ru(4) bond. On the basis of the non-hydrogen framework, HYDEX[10] also predicts two different types of site for the hydrido ligands of (**5**), with the calculated position of H(1) being closer to Au(2) than that of H(2). However, the available data are, of necessity, rather imprecise and cannot unambiguously define the bonding mode of the hydrido ligands in (**5**).

Figure 3 compares the internuclear metal–metal distances within the skeletal frameworks of (**1**), (**2**), and (**5**). It can be seen that the two coinage metals are in close contact in each case. Rather surprisingly, as the separations between the atoms in metallic gold (2.884 Å)[11] and silver (2.889 Å)[12] are very similar, Au(1)–Au(2) [2.791(1) Å] is significantly shorter than Ag(1)–Ag(2) [2.857(1) Å]. However, as expected, both Au(1)–Au(2) and Ag(1)–Ag(2) are considerably longer than Cu(1)–Cu(2) [2.699(2) Å]. The value of Au(1)–Au(2) in (**5**) lies nearer to the lower end of the range previously observed in heteronuclear cluster compounds [2.590(2)—3.176(1) Å].[2,3,13] Few values for Ag–Ag or Cu–Cu distances in mixed-metal clusters have been reported. However, the Ag(1)–Ag(2) separation in (**2**) lies very near to the lower end of the range of

Table 3. Selected bond lengths (Å) and angles (°), with estimated standard deviations in parentheses, for $[Cu_2Ru_4(\mu_3\text{-}H)_2(CO)_{12}(PPh_3)_2]$ (**1**)

H(1)–Ru(4)	1.810(52)	H(1)–Ru(1)	1.758(43)	Ru(3)–C(7)	1.893(9)	Ru(3)–C(8)	1.898(8)
H(1)–Cu(2)	1.656(55)	H(2)–Ru(1)	1.823(69)	Ru(3)–C(9)	1.893(10)	Cu(1)–Cu(2)	2.699(2)
H(2)–Ru(3)	1.772(45)	H(2)–Cu(2)	1.528(70)	Cu(1)–P(1)	2.266(2)	Cu(2)–P(2)	2.202(3)
Ru(2)–Ru(4)	2.800(2)	Ru(2)–Ru(1)	2.790(2)	P(1)–C(111)	1.816(8)	P(1)–C(121)	1.830(9)
Ru(2)–Ru(3)	2.795(2)	Ru(2)–C(5)	1.892(11)	P(1)–C(131)	1.828(7)	P(2)–C(211)	1.906(8)
Ru(2)–C(4)	1.894(11)	Ru(2)–C(6)	1.879(9)	P(2)–C(261)	1.714(8)	P(2)–C(221)	1.885(11)
Ru(4)–Ru(1)	2.947(2)	Ru(4)–Ru(3)	2.923(2)	P(2)–C(231)	1.852(8)	P(2)–C(241)	1.854(9)
Ru(4)–Cu(1)	2.699(2)	Ru(4)–Cu(2)	2.674(2)	P(2)–C(251)	1.735(10)	C(5)–O(5)	1.139(13)
Ru(4)–C(10)	1.887(7)	Ru(4)–C(12)	1.888(8)	C(4)–O(4)	1.130(14)	C(6)–O(6)	1.154(12)
Ru(4)–C(11)	1.920(8)	Ru(1)–Ru(3)	2.966(2)	C(10)–O(10)	1.134(9)	C(12)–O(12)	1.151(9)
Ru(1)–Cu(2)	2.809(2)	Ru(1)–C(2)	1.897(8)	C(11)–O(11)	1.129(10)	C(2)–O(2)	1.127(10)
Ru(1)–C(3)	1.881(8)	Ru(1)–C(1)	1.939(10)	C(3)–O(3)	1.154(10)	C(1)–O(1)	1.119(12)
Ru(3)–Cu(1)	2.679(2)	Ru(3)–Cu(2)	2.671(2)	C(7)–O(7)	1.122(10)	C(8)–O(8)	1.149(10)
				C(9)–O(9)	1.130(13)		

Ru(4)–H(1)–Ru(1)	111.4(34)	Ru(4)–H(1)–Cu(2)	100.9(22)	Cu(2)–Ru(1)–C(1)	77.8(2)	C(2)–Ru(1)–C(1)	96.3(4)
Ru(1)–H(1)–Cu(2)	110.7(24)	Ru(1)–H(2)–Ru(3)	111.2(41)	C(3)–Ru(1)–C(1)	94.3(4)	H(2)–Ru(3)–Ru(2)	92.2(25)
Ru(1)–H(2)–Cu(2)	113.6(30)	Ru(3)–H(2)–Cu(2)	107.8(30)	H(2)–Ru(3)–Ru(4)	70.2(20)	Ru(2)–Ru(3)–Ru(4)	58.6(1)
Ru(4)–Ru(2)–Ru(1)	63.6(1)	Ru(4)–Ru(2)–Ru(3)	63.0(1)	H(2)–Ru(3)–Ru(1)	35.0(25)	Ru(2)–Ru(3)–Ru(1)	57.8(1)
Ru(1)–Ru(2)–Ru(3)	64.2(1)	Ru(4)–Ru(2)–C(5)	100.6(4)	Ru(4)–Ru(3)–Ru(1)	60.1(1)	H(2)–Ru(3)–Cu(1)	93.4(21)
Ru(1)–Ru(2)–C(5)	163.1(4)	Ru(3)–Ru(2)–C(5)	104.1(3)	Ru(2)–Ru(3)–Cu(1)	108.7(1)	Ru(4)–Ru(3)–Cu(1)	57.4(1)
Ru(4)–Ru(2)–C(4)	156.2(3)	Ru(1)–Ru(2)–C(4)	100.3(3)	Ru(1)–Ru(3)–Cu(1)	109.2(1)	H(2)–Ru(3)–Cu(2)	33.0(22)
Ru(3)–Ru(2)–C(4)	94.6(3)	C(5)–Ru(2)–C(4)	92.5(5)	Ru(2)–Ru(3)–Cu(2)	105.0(1)	Ru(4)–Ru(3)–Cu(2)	56.9(1)
Ru(4)–Ru(2)–C(6)	105.2(3)	Ru(1)–Ru(2)–C(6)	97.8(3)	Ru(1)–Ru(3)–Cu(2)	59.5(1)	Cu(1)–Ru(3)–Cu(2)	60.6(1)
Ru(3)–Ru(2)–C(6)	161.2(4)	C(5)–Ru(2)–C(6)	92.3(4)	H(2)–Ru(3)–C(7)	162.4(20)	Ru(2)–Ru(3)–C(7)	79.4(3)
C(4)–Ru(2)–C(6)	93.9(4)	H(1)–Ru(4)–Ru(2)	91.6(17)	Ru(4)–Ru(3)–C(7)	92.3(2)	Ru(1)–Ru(3)–C(7)	136.5(2)
H(1)–Ru(4)–Ru(1)	33.7(17)	Ru(2)–Ru(4)–Ru(1)	58.0(1)	Cu(1)–Ru(3)–C(7)	75.1(3)	Cu(2)–Ru(3)–C(7)	134.7(3)
H(1)–Ru(4)–Ru(3)	73.7(15)	Ru(2)–Ru(4)–Ru(3)	58.4(1)	H(2)–Ru(3)–C(8)	87.3(26)	Ru(2)–Ru(3)–C(8)	175.5(2)
Ru(1)–Ru(4)–Ru(3)	60.7(1)	H(1)–Ru(4)–Cu(1)	97.6(16)	Ru(4)–Ru(3)–C(8)	117.1(2)	Ru(1)–Ru(3)–C(8)	122.0(2)
Ru(2)–Ru(4)–Cu(1)	107.9(1)	Ru(1)–Ru(4)–Cu(1)	109.2(1)	Cu(1)–Ru(3)–C(8)	66.9(2)	Cu(2)–Ru(3)–C(8)	72.2(2)
Ru(3)–Ru(4)–Cu(1)	56.8(1)	H(1)–Ru(4)–Cu(2)	37.4(16)	C(7)–Ru(3)–C(8)	99.9(3)	H(2)–Ru(3)–C(9)	104.3(20)
Ru(2)–Ru(4)–Cu(2)	104.8(1)	Ru(1)–Ru(4)–Cu(2)	59.7(1)	Ru(2)–Ru(3)–C(9)	91.4(3)	Ru(4)–Ru(3)–C(9)	148.4(3)
Ru(3)–Ru(4)–Cu(2)	56.8(1)	Cu(1)–Ru(4)–Cu(2)	60.3(1)	Ru(1)–Ru(3)–C(9)	96.9(3)	Cu(1)–Ru(3)–C(9)	152.8(3)
H(1)–Ru(4)–C(10)	168.2(15)	Ru(2)–Ru(4)–C(10)	85.4(3)	Cu(2)–Ru(3)–C(9)	132.7(4)	C(7)–Ru(3)–C(9)	91.4(4)
Ru(1)–Ru(4)–C(10)	142.6(3)	Ru(3)–Ru(4)–C(10)	95.1(2)	C(8)–Ru(3)–C(9)	93.1(4)	Ru(4)–Cu(1)–Ru(3)	65.9(1)
Cu(1)–Ru(4)–C(10)	72.5(2)	Cu(2)–Ru(4)–C(10)	132.7(2)	Ru(4)–Cu(1)–Cu(2)	59.4(1)	Ru(3)–Cu(1)–Cu(2)	59.6(1)
H(1)–Ru(4)–C(12)	101.0(16)	Ru(2)–Ru(4)–C(12)	83.4(3)	Ru(4)–Cu(1)–P(1)	139.4(1)	Ru(3)–Cu(1)–P(1)	147.1(1)
Ru(1)–Ru(4)–C(12)	92.9(2)	Ru(3)–Ru(4)–C(12)	140.8(3)	Cu(2)–Cu(1)–P(1)	144.3(1)	H(1)–Cu(2)–H(2)	69.4(30)
Cu(1)–Ru(4)–C(12)	157.9(2)	Cu(2)–Ru(4)–C(12)	136.4(3)	H(1)–Cu(2)–Ru(4)	41.6(17)	H(2)–Cu(2)–Ru(4)	80.7(26)
C(10)–Ru(4)–C(12)	90.1(3)	H(1)–Ru(4)–C(11)	83.9(17)	H(1)–Cu(2)–Ru(1)	35.8(14)	H(2)–Cu(2)–Ru(1)	36.5(22)
Ru(2)–Ru(4)–C(11)	175.2(2)	Ru(1)–Ru(4)–C(11)	117.4(2)	Ru(4)–Cu(2)–Ru(1)	65.0(1)	H(1)–Cu(2)–Ru(3)	83.3(20)
Ru(3)–Ru(4)–C(11)	121.6(2)	Cu(1)–Ru(4)–C(11)	74.5(2)	H(2)–Cu(2)–Ru(3)	39.2(16)	Ru(4)–Cu(2)–Ru(3)	66.3(1)
Cu(2)–Ru(4)–C(11)	72.6(2)	C(10)–Ru(4)–C(11)	99.3(4)	Ru(1)–Cu(2)–Ru(3)	65.5(1)	H(1)–Cu(2)–Cu(1)	101.8(18)
C(12)–Ru(4)–C(11)	95.7(4)	H(1)–Ru(1)–H(2)	60.9(25)	H(2)–Cu(2)–Cu(1)	98.8(16)	Ru(4)–Cu(2)–Cu(1)	60.3(1)
H(1)–Ru(1)–Ru(2)	93.1(20)	H(2)–Ru(1)–Ru(2)	91.2(18)	Ru(1)–Cu(2)–Cu(1)	113.4(1)	Ru(3)–Cu(2)–Cu(1)	59.8(1)
H(1)–Ru(1)–Ru(4)	34.9(20)	H(2)–Ru(1)–Ru(4)	69.0(19)	H(1)–Cu(2)–P(2)	128.6(20)	H(2)–Cu(2)–P(2)	127.7(24)
Ru(2)–Ru(1)–Ru(4)	58.3(1)	H(1)–Ru(1)–Ru(3)	73.0(16)	Ru(4)–Cu(2)–P(2)	148.6(1)	Ru(1)–Cu(2)–P(2)	127.9(1)
H(2)–Ru(1)–Ru(3)	33.9(18)	Ru(2)–Ru(1)–Ru(3)	58.0(1)	Ru(3)–Cu(2)–P(2)	143.4(1)	Cu(1)–Cu(2)–P(2)	118.6(1)
Ru(4)–Ru(1)–Ru(3)	59.2(1)	H(1)–Ru(1)–Cu(2)	33.5(17)	Cu(1)–P(1)–C(111)	114.3(3)	Cu(1)–P(1)–C(121)	120.4(2)
H(2)–Ru(1)–Cu(2)	29.9(19)	Ru(2)–Ru(1)–Cu(2)	101.6(1)	C(111)–P(1)–C(121)	102.4(3)	Cu(1)–P(1)–C(131)	109.6(2)
Ru(4)–Ru(1)–Cu(2)	55.3(1)	Ru(3)–Ru(1)–Cu(2)	55.0(1)	C(111)–P(1)–C(131)	104.8(3)	C(121)–P(1)–C(131)	103.8(4)
H(1)–Ru(1)–C(2)	166.6(16)	H(2)–Ru(1)–C(2)	106.1(20)	Cu(2)–P(2)–C(211)	117.5(3)	Cu(2)–P(2)–C(261)	113.8(4)
Ru(2)–Ru(1)–C(2)	83.8(3)	Ru(4)–Ru(1)–C(2)	141.0(3)	Cu(2)–P(2)–C(221)	115.0(3)	Cu(2)–P(2)–C(231)	112.9(4)
Ru(3)–Ru(1)–C(2)	94.4(3)	Cu(2)–Ru(1)–C(2)	134.6(3)	Cu(2)–P(2)–C(241)	112.1(4)	Cu(2)–P(2)–C(251)	114.6(4)
H(1)–Ru(1)–C(3)	99.8(16)	H(2)–Ru(1)–C(3)	160.5(19)	Ru(2)–C(5)–O(5)	177.3(11)	Ru(2)–C(4)–O(4)	176.9(9)
Ru(2)–Ru(1)–C(3)	86.5(3)	Ru(4)–Ru(1)–C(3)	93.5(2)	Ru(2)–C(6)–O(6)	176.9(10)	Ru(4)–C(10)–O(10)	175.3(6)
Ru(3)–Ru(1)–C(3)	142.5(3)	Cu(2)–Ru(1)–C(3)	132.1(3)	Ru(4)–C(12)–O(12)	176.5(8)	Ru(4)–C(11)–O(11)	172.0(6)
C(2)–Ru(1)–C(3)	92.9(4)	H(1)–Ru(1)–C(1)	86.6(20)	Ru(1)–C(2)–O(2)	176.1(10)	Ru(1)–C(3)–O(3)	175.8(9)
H(2)–Ru(1)–C(1)	88.0(19)	Ru(2)–Ru(1)–C(1)	179.2(2)	Ru(1)–C(1)–O(1)	171.4(8)	Ru(3)–C(7)–O(7)	174.3(6)
Ru(4)–Ru(1)–C(1)	121.4(2)	Ru(3)–Ru(1)–C(1)	121.2(2)	Ru(3)–C(8)–O(8)	170.1(7)	Ru(3)–C(9)–O(9)	177.5(10)

Ag–Ag distances which are considered to indicate bonding in $[Ag_6\{Fe(CO)_4\}_3\{CH(PPh_2)_3\}]$ [2.817(1)—3.065(1) Å][14] and it is also comparable to the shorter Ag–Ag separations in $[Ag_{12}Au_{13}Cl_6(PPh_3)_{12}]^{m+}$ [2.87(3)—3.54(3) Å].[15] Moreover, the Cu(1)–Cu(2) separation in (**1**) is similar to the Cu–Cu distance in $[Cu_2Ru_6C(CO)_{16}(NCMe)_2]$ [variously reported as 2.689, 2.693(1), and 2.691(1) Å][16] and it is also comparable to the longer Cu–Cu separations in the homonuclear species $[Cu_6H_6(PR_3)_6]$ (R = Ph or *p*-tolyl) [2.632(6)—2.749(4) Å].[17]

As expected,[1] the lengths of the three unbridged Ru–Ru vectors [Ru(1)–Ru(2), Ru(2)–Ru(3), and Ru(2)–Ru(4)] in the Ru_4 tetrahedra of (**1**), (**2**), and (**5**) are altered very little by the change in coinage metals and they are considerably shorter than the three Ru–Ru edges capped by $M(PPh_3)$ moieties or hydrido ligands [Ru(1)–Ru(3), Ru(1)–Ru(4), and Ru(3)–Ru(4)]. Of these latter three Ru–Ru separations, the length of the vector [Ru(3)–Ru(4)] which acts as a common edge for the two capping coinage metal fragments is altered much more

Table 4. Selected bond lengths (Å) and angles (°), with estimated standard deviations in parentheses, for $[Ag_2Ru_4(\mu_3\text{-}H)_2(CO)_{12}(PPh_3)_2]$ (**2**)

H(1)–Ag(2)	1.692(91)	H(1)–Ru(1)	1.765(49)	Ru(2)–C(6)	1.873(14)	Ru(3)–Ru(4)	2.961(1)
H(1)–Ru(3)	1.802(85)	H(2)–Ag(2)	1.757(95)	Ru(3)–C(7)	1.879(9)	Ru(3)–C(8)	1.924(11)
H(2)–Ru(1)	1.754(87)	H(2)–Ru(4)	1.835(47)	Ru(3)–C(9)	1.883(10)	Ru(4)–C(10)	1.883(10)
Ag(1)–Ag(2)	2.857(1)	Ag(1)–Ru(3)	2.855(1)	Ru(4)–C(11)	1.898(11)	Ru(4)–C(12)	1.876(12)
Ag(1)–Ru(4)	2.842(1)	Ag(1)–P(1)	2.421(3)	P(1)–C(111)	1.823(11)	P(1)–C(121)	1.809(11)
Ag(2)–Ru(1)	2.980(1)	Ag(2)–Ru(3)	2.880(1)	P(1)–C(131)	1.835(10)	P(2)–C(211)	1.817(11)
Ag(2)–Ru(4)	2.913(1)	Ag(2)–P(2)	2.382(4)	P(2)–C(221)	1.829(10)	P(2)–C(231)	1.811(10)
Ru(1)–Ru(2)	2.785(1)	Ru(1)–Ru(3)	2.967(1)	C(1)–O(1)	1.138(15)	C(2)–O(2)	1.139(13)
Ru(1)–Ru(4)	2.979(1)	Ru(1)–C(1)	1.928(12)	C(3)–O(3)	1.124(12)	C(4)–O(4)	1.145(15)
Ru(1)–C(2)	1.875(11)	Ru(1)–C(3)	1.879(10)	C(5)–O(5)	1.138(15)	C(6)–O(6)	1.134(17)
Ru(2)–Ru(3)	2.806(1)	Ru(2)–Ru(4)	2.799(1)	C(7)–O(7)	1.135(11)	C(8)–O(8)	1.141(13)
Ru(2)–C(4)	1.898(11)	Ru(2)–C(5)	1.884(11)	C(9)–O(9)	1.130(12)	C(10)–O(10)	1.140(12)
				C(11)–O(11)	1.144(13)	C(12)–O(12)	1.138(15)

Ag(2)–H(1)–Ru(1)	119.1(40)	Ag(2)–H(1)–Ru(3)	111.0(31)	H(1)–Ru(3)–Ru(2)	89.9(24)	Ag(1)–Ru(3)–Ru(2)	109.9(1)
Ru(1)–H(1)–Ru(3)	112.5(54)	Ag(2)–H(2)–Ru(1)	116.2(33)	Ag(2)–Ru(3)–Ru(2)	107.3(1)	Ru(1)–Ru(3)–Ru(2)	57.6(1)
Ag(2)–H(2)–Ru(4)	108.4(37)	Ru(1)–H(2)–Ru(4)	112.2(51)	H(1)–Ru(3)–Ru(4)	68.3(24)	Ag(1)–Ru(3)–Ru(4)	58.5(1)
Ag(2)–Ag(1)–Ru(3)	60.6(1)	Ag(2)–Ag(1)–Ru(4)	61.5(1)	Ag(2)–Ru(3)–Ru(4)	59.8(1)	Ru(1)–Ru(3)–Ru(4)	60.3(1)
Ru(3)–Ag(1)–Ru(4)	62.6(1)	Ag(2)–Ag(1)–P(1)	140.9(1)	Ru(2)–Ru(3)–Ru(4)	58.0(1)	H(1)–Ru(3)–C(7)	160.7(25)
Ru(3)–Ag(1)–P(1)	140.6(1)	Ru(4)–Ag(1)–P(1)	149.1(1)	Ag(1)–Ru(3)–C(7)	71.5(3)	Ag(2)–Ru(3)–C(7)	131.2(3)
H(1)–Ag(2)–H(2)	57.5(33)	H(1)–Ag(2)–Ag(1)	94.4(27)	Ru(1)–Ru(3)–C(7)	142.8(3)	Ru(2)–Ru(3)–C(7)	86.5(4)
H(2)–Ag(2)–Ag(1)	95.2(16)	H(1)–Ag(2)–Ru(1)	31.2(16)	Ru(4)–Ru(3)–C(7)	93.9(2)	H(1)–Ru(3)–C(8)	86.8(24)
H(2)–Ag(2)–Ru(1)	31.9(22)	Ag(1)–Ag(2)–Ru(1)	109.0(1)	Ag(1)–Ru(3)–C(8)	74.0(3)	Ag(2)–Ru(3)–C(8)	71.8(3)
H(1)–Ag(2)–Ru(3)	35.7(23)	H(2)–Ag(2)–Ru(3)	72.7(27)	Ru(1)–Ru(3)–C(8)	118.5(3)	Ru(2)–Ru(3)–C(8)	174.9(3)
Ag(1)–Ag(2)–Ru(3)	59.7(1)	Ru(1)–Ag(2)–Ru(3)	60.8(1)	Ru(4)–Ru(3)–C(8)	123.9(3)	C(7)–Ru(3)–C(8)	97.9(4)
H(1)–Ag(2)–Ru(4)	70.6(29)	H(2)–Ag(2)–Ru(4)	36.7(15)	H(1)–Ru(3)–C(9)	107.5(25)	Ag(1)–Ru(3)–C(9)	157.8(3)
Ag(1)–Ag(2)–Ru(4)	59.0(1)	Ru(1)–Ag(2)–Ru(4)	60.7(1)	Ag(2)–Ru(3)–C(9)	137.0(3)	Ru(1)–Ru(3)–C(9)	92.8(3)
Ru(3)–Ag(2)–Ru(4)	61.5(1)	H(1)–Ag(2)–P(2)	142.2(30)	Ru(2)–Ru(3)–C(9)	81.1(4)	Ru(4)–Ru(3)–C(9)	138.4(3)
H(2)–Ag(2)–P(2)	132.0(25)	Ag(1)–Ag(2)–P(2)	117.4(1)	C(7)–Ru(3)–C(9)	90.6(4)	C(8)–Ru(3)–C(9)	96.3(5)
Ru(1)–Ag(2)–P(2)	133.1(1)	Ru(3)–Ag(2)–P(2)	153.7(1)	H(2)–Ru(4)–Ag(1)	93.9(28)	H(2)–Ru(4)–Ag(2)	34.9(29)
Ru(4)–Ag(2)–P(2)	142.5(1)	H(1)–Ru(1)–H(2)	56.3(36)	Ag(1)–Ru(4)–Ag(2)	59.5(1)	H(2)–Ru(4)–Ru(1)	33.0(31)
H(1)–Ru(1)–Ag(2)	29.7(29)	H(2)–Ru(1)–Ag(2)	31.9(26)	Ag(1)–Ru(4)–Ru(1)	109.4(1)	Ag(2)–Ru(4)–Ru(1)	60.8(1)
H(1)–Ru(1)–Ru(2)	91.4(33)	H(2)–Ru(1)–Ru(2)	92.2(22)	H(2)–Ru(4)–Ru(2)	90.0(31)	Ag(1)–Ru(4)–Ru(2)	110.5(1)
Ag(2)–Ru(1)–Ru(2)	105.1(1)	H(1)–Ru(1)–Ru(3)	34.1(33)	Ag(2)–Ru(4)–Ru(2)	106.6(1)	Ru(1)–Ru(4)–Ru(2)	57.5(1)
H(2)–Ru(1)–Ru(3)	70.3(25)	Ag(2)–Ru(1)–Ru(3)	57.9(1)	H(2)–Ru(4)–Ru(3)	69.7(24)	Ag(1)–Ru(4)–Ru(3)	58.9(1)
Ru(2)–Ru(1)–Ru(3)	58.3(1)	H(1)–Ru(1)–Ru(4)	68.1(26)	Ag(2)–Ru(4)–Ru(3)	58.7(1)	Ru(1)–Ru(4)–Ru(3)	59.9(1)
H(2)–Ru(1)–Ru(4)	34.7(22)	Ag(2)–Ru(1)–Ru(4)	58.5(1)	Ru(2)–Ru(4)–Ru(3)	58.2(1)	H(2)–Ru(4)–C(10)	159.9(24)
Ru(2)–Ru(1)–Ru(4)	58.0(1)	Ru(3)–Ru(1)–Ru(4)	59.7(1)	Ag(1)–Ru(4)–C(10)	72.1(4)	Ag(2)–Ru(4)–C(10)	131.0(3)
H(1)–Ru(1)–C(1)	88.2(33)	H(2)–Ru(1)–C(1)	86.5(23)	Ru(1)–Ru(4)–C(10)	137.8(3)	Ru(2)–Ru(4)–C(10)	81.9(3)
Ag(2)–Ru(1)–C(1)	73.9(3)	Ru(2)–Ru(1)–C(1)	178.6(3)	Ru(3)–Ru(4)–C(10)	90.5(3)	H(2)–Ru(4)–C(11)	88.0(31)
Ru(3)–Ru(1)–C(1)	121.5(3)	Ru(4)–Ru(1)–C(1)	120.7(3)	Ag(1)–Ru(4)–C(11)	69.0(3)	Ag(2)–Ru(4)–C(11)	71.4(3)
H(1)–Ru(1)–C(2)	105.3(26)	H(2)–Ru(1)–C(2)	161.6(26)	Ru(1)–Ru(4)–C(11)	120.5(3)	Ru(2)–Ru(4)–C(11)	177.9(3)
Ag(2)–Ru(1)–C(2)	130.9(3)	Ru(2)–Ru(1)–C(2)	87.9(4)	Ru(3)–Ru(4)–C(11)	120.4(3)	C(10)–Ru(4)–C(11)	99.9(4)
Ru(3)–Ru(1)–C(2)	94.3(3)	Ru(4)–Ru(1)–C(2)	144.1(3)	H(2)–Ru(4)–C(12)	107.4(26)	Ag(1)–Ru(4)–C(12)	151.9(3)
C(1)–Ru(1)–C(2)	93.4(5)	H(1)–Ru(1)–C(3)	160.2(25)	Ag(2)–Ru(4)–C(12)	136.8(4)	Ru(1)–Ru(4)–C(12)	98.3(3)
H(2)–Ru(1)–C(3)	104.5(26)	Ag(2)–Ru(1)–C(3)	133.8(3)	Ru(2)–Ru(4)–C(12)	88.0(4)	Ru(3)–Ru(4)–C(12)	145.7(4)
Ru(2)–Ru(1)–C(3)	84.2(4)	Ru(3)–Ru(1)–C(3)	141.2(4)	C(10)–Ru(4)–C(12)	90.7(5)	C(11)–Ru(4)–C(12)	93.2(5)
Ru(4)–Ru(1)–C(3)	93.4(3)	C(1)–Ru(1)–C(3)	95.7(5)	Ag(1)–P(1)–C(111)	112.6(4)	Ag(1)–P(1)–C(121)	119.1(3)
C(2)–Ru(1)–C(3)	93.9(5)	Ru(1)–Ru(2)–Ru(3)	64.1(1)	C(111)–P(1)–C(121)	104.2(4)	Ag(1)–P(1)–C(131)	109.5(3)
Ru(1)–Ru(2)–Ru(4)	64.5(1)	Ru(3)–Ru(2)–Ru(4)	63.8(1)	C(111)–P(1)–C(131)	105.3(5)	C(121)–P(1)–C(131)	105.0(5)
Ru(1)–Ru(2)–C(4)	97.8(4)	Ru(3)–Ru(2)–C(4)	104.8(4)	Ag(2)–P(2)–C(211)	111.9(4)	Ag(2)–P(2)–C(221)	112.7(5)
Ru(4)–Ru(2)–C(4)	161.6(4)	Ru(1)–Ru(2)–C(5)	162.5(4)	C(211)–P(2)–C(221)	105.4(5)	Ag(2)–P(2)–C(231)	116.3(4)
Ru(3)–Ru(2)–C(5)	100.0(4)	Ru(4)–Ru(2)–C(5)	102.8(4)	C(211)–P(2)–C(231)	102.5(5)	C(221)–P(2)–C(231)	107.0(5)
C(4)–Ru(2)–C(5)	93.2(5)	Ru(1)–Ru(2)–C(6)	101.9(4)	Ru(1)–C(1)–O(1)	172.0(10)	Ru(1)–C(2)–O(2)	175.2(11)
Ru(3)–Ru(2)–C(6)	159.1(4)	Ru(4)–Ru(2)–C(6)	96.6(4)	Ru(1)–C(3)–O(3)	176.2(10)	Ru(2)–C(4)–O(4)	177.0(12)
C(4)–Ru(2)–C(6)	92.1(5)	C(5)–Ru(2)–C(6)	91.1(6)	Ru(2)–C(5)–O(5)	175.8(12)	Ru(2)–C(6)–O(6)	178.4(14)
H(1)–Ru(3)–Ag(1)	92.1(25)	H(1)–Ru(3)–Ag(2)	33.3(25)	Ru(3)–C(7)–O(7)	175.6(7)	Ru(3)–C(8)–O(8)	171.6(10)
Ag(1)–Ru(3)–Ag(2)	59.7(1)	H(1)–Ru(3)–Ru(1)	33.3(23)	Ru(3)–C(9)–O(9)	176.0(8)	Ru(4)–C(10)–O(10)	175.9(7)
Ag(1)–Ru(3)–Ru(1)	109.4(1)	Ag(2)–Ru(3)–Ru(1)	61.3(1)	Ru(4)–C(11)–O(11)	171.0(10)	Ru(4)–C(12)–O(12)	176.9(13)

extensively by the changes in Group 1B metal than that of the other two edges. The Cu–Ru separations in (**1**) [2.671(2)—2.809(2) Å] are all significantly shorter than the corresponding Ag–Ru [2.842(1)—2.980(1) Å] and Au–Ru [2.840(1)—3.091(1) Å] distances in (**2**) and (**5**), respectively, but there is generally relatively little difference in length between equivalent M–Ru edges in (**2**) and (**5**). For all three clusters, the M(2)–Ru(1) separation is the longest M–Ru distance and this value is considerably increased (*ca.* 0.11 Å) by the change from M = Ag to Au.

Interestingly, the previously reported[18] osmium analogue of (**5**) exists as two different isomeric forms, but, unfortunately, only one of these isomers (**A**) has been structurally characterized by an *X*-ray diffraction study and no evidence to suggest the structure of the second isomer (**B**) is available. The i.r. spectrum of isomer (**A**)[18] is very similar to that of (**5**) (Table 1) and the *X*-ray diffraction analysis confirms that the metal core geometry of the gold–osmium cluster is very closely related to the structure of (**5**), although it is thought[18] that the equivalent Au–Os separation [3.159(4) Å] to Au(2)–Ru(1) in (**5**) may be too long

to be considered as a formal bond. Rather surprisingly, the Au–Au distance in the osmium species [2.793(4) Å] is identical to that in (**5**) [2.791(1) Å], within the error limits. In contrast to those in (**5**), the two hydrido ligands in $[Au_2Os_4(\mu\text{-}H)_2(CO)_{12}(PPh_3)_2]$ are thought[18] to edge-bridge the two Os–Os vectors equivalent to Ru(1)–Ru(3) and Ru(1)–Ru(4). Unlike the gold–osmium species, no evidence for more than one isomeric form was found in the solid state or in solution for (**1**), (**2**), or (**5**).

As well as (**1**), (**2**), (**5**), and $[Au_2Os_4(\mu\text{-}H)_2(CO)_{12}(PPh_3)_2]$,[18] a number of other heteronuclear clusters are known[3,16,19–23] to exhibit structures in which a Group 1B metal caps a triangular face of a polyhedron containing other different transition metals, and a second coinage metal, in close contact with the first, caps one face of the tetrahedron so formed. The copper–ruthenium species $[Cu_2Ru_6C(CO)_{16}(NCMe)_2]$[16] contains this coinage metal arrangement, as do the gold mixed-metal clusters $[Au_2M_3(\mu_3\text{-}S)(CO)_8L(PPh_3)_2]$ (M = Fe, L = CO;[19] M = Ru, L = CO[3,20] or PPh_3[3]), $[Au_2Ru_3(\mu_3\text{-}C{\equiv}CH\text{-}Bu^t)(CO)_9(PPh_3)_2]$,[21] $[Au_2Co_2Ru_2(CO)_{12}(PPh_3)_2]$,[19] $[Au_2CoRu_3(\mu\text{-}H)(CO)_{12}(PPh_3)_2]$,[22] and $[Au_2Ru_5WC(CO)_{17}(PEt_3)_2]$.[23]

Having established the molecular structures of (**1**), (**2**), and (**5**), it is possible to interpret the variable-temperature n.m.r. spectra of these species (Table 2). A singlet, broadened by quadrupolar effects from the copper atoms,[1,24] is observed in the ambient temperature $^{31}P\text{-}\{^1H\}$ n.m.r. spectrum of (**1**). As there are two distinct phosphorus environments in the ground-state structure of the cluster (Figure 1), it is clear that, at ambient temperature in solution, (**1**) is undergoing some fluxional process which exchanges the PPh_3 groups between the two different sites. At −90 °C, however, two singlets are visible in the $^{31}P\text{-}\{^1H\}$ n.m.r. spectrum, consistent with the solid-state structure. The high-field hydrido ligand signal in the ambient temperature ^1H n.m.r. spectrum of (**1**) is a triplet [J(PH) 5 Hz], showing coupling to two equivalent phosphorus atoms. However, at −90 °C, the ^1H n.m.r. hydrido ligand peak is a doublet [J(PH) 12 Hz] and this observation is consistent with the ground-state geometry, in which P(2) would be expected to show coupling to the hydrido ligands, but P(1) would not. The ^1H n.m.r. hydrido ligand signal for (**1**) retains the $^{31}P\text{–}^1H$ coupling throughout the temperature range from −90 °C to room temperature, thus demonstrating that the fluxional process which averages the phosphorus environments must be intramolecular. However, no examples of intramolecular exchange of phosphine ligands between metal atoms in cluster compounds at ambient temperature have been previously reported. Therefore, we postulate that the actual metal framework of (**1**) is in motion and that it is the two copper atoms which are exchanging between the two distinct sites, taking the attached PPh_3 groups with them. Similar intramolecular metal core arrangements have been previously proposed[3–5,23] for a number of heteronuclear clusters containing two or three gold atoms and such a fluxional process has very recently been directly observed[25] in the silver–ruthenium species $[Ag_2Ru_4(\mu_3\text{-}H)_2\{\mu\text{-}Ph_2P(CH_2)_nPPh_2\}(CO)_{12}]$ (n = 1, 2, or 4) by INEPT $^{109}Ag\text{-}\{^1H\}$ n.m.r. experiments.

The gold–ruthenium cluster (**5**) exhibits the same dynamic behaviour as (**1**). At ambient temperature, a singlet is visible in the $^{31}P\text{-}\{^1H\}$ n.m.r. spectrum and the ^1H n.m.r. hydrido ligand signal is a triplet [J(PH) 5 Hz]. However, spectra consistent with the ground-state structure cannot be obtained for (**5**), even at −90 °C, although both the $^{31}P\text{-}\{^1H\}$ n.m.r. signal and the ^1H n.m.r. hydrido ligand peak are very broad at this temperature.

In the case of the silver–ruthenium cluster (**2**), the interpretation of the n.m.r. spectra is complicated by a second fluxional process. At ambient temperature, the $^{31}P\text{-}\{^1H\}$ n.m.r. signal consists of two very broad peaks and the high field hydrido ligand peak in the ^1H n.m.r. spectrum is a rather broad triplet [$J(AgH)_{av}$ 12 Hz], which shows no $^{31}P\text{–}^1H$ coupling. However, at −50 °C, $^{31}P\text{–}^1H$ coupling is observed and the hydrido ligand peak appears as a triplet of triplets [$J(AgH)_{av}$ 14, J(PH) 5 Hz]. These observations suggest that, at ambient temperature in $CDCl_3$ or CD_2Cl_2 solution, (**2**) is undergoing a fluxional process involving intermolecular exchange of PPh_3 groups between clusters in addition to the intramolecular metal core rearrangement proposed for (**1**) and (**5**) and that only the latter process still operates at −50 °C. The free energies of activation for the two dynamic processes are such that it is impossible to obtain a sharp $^{31}P\text{-}\{^1H\}$ n.m.r. spectrum for the situation where only the intramolecular metal core rearrangement is in progress. Supporting the idea of phosphine ligand exchange, when one equivalent of free PPh_3 is added to a sample of (**2**) in $CDCl_3$ or CD_2Cl_2 solution, the $^{31}P\text{-}\{^1H\}$ n.m.r. spectrum of the mixture shows only one broad peak, with a chemical shift intermediate between that of the $Ag(PPh_3)$ moieties in (**2**) and that of the free ligand. The detection of only one signal for an averaged PPh_3 environment demonstrates that PPh_3 groups bonded to the silver atoms in (**2**) can exchange with the free ligand *in solution*. Similar lability of phosphine groups bonded to silver atoms has been previously reported for other heteronuclear cluster compounds.[1]

At −90 °C, ^1H and $^{31}P\text{-}\{^1H\}$ n.m.r. spectra consistent with the ground-state structure of (**2**) can be obtained. The high-field hydrido ligand signal is a doublet of doublets, due to Ag(2) and P(2) coupling to the hydrido ligands [$J(AgH)_{av}$ 27, J(PH) 9 Hz]. The $^{31}P\text{-}\{^1H\}$ n.m.r. spectrum shows two phosphorus environments. The resonance for each environment is split into two doublets by the large $^{109}Ag\text{–}^{31}P$ and $^{107}Ag\text{–}^{31}P$ couplings through one bond, and these doublets are all further split by an extra, small $^{107,109}Ag\text{–}^{31}P$ coupling through two bonds. The magnitudes of the latter couplings are not sufficient to allow the two separate contributions from ^{107}Ag and ^{109}Ag to be resolved.

It is interesting to compare the free energies of activation ($\Delta G^{\ddagger}$) for the intramolecular metal core rearrangements of (**1**), (**2**), and (**5**). For (**1**) and (**2**), coalescence temperatures of -45 ± 5 and -65 ± 5 °C give values of $\Delta G^{\ddagger}$ at the coalescence temperature of 43 ± 1 and 40 ± 1 kJ mol^{-1}, respectively. In the case of (**1**), band-shape analysis of the $^{31}P\text{-}\{^1H\}$ n.m.r. spectra affords a more accurate value for $\Delta G^{\ddagger}$, 40.9 ± 0.3 kJ mol^{-1} at 298 K.[26] However, it is not possible to apply the technique to (**2**) because of the additional broadening of the spectra caused by the intermolecular PPh_3 exchange. Ground-state spectra cannot be obtained for (**5**), but a value for $\Delta G^{\ddagger}$ at the coalescence temperature (*ca.* −90 °C) can be estimated by assuming that the difference in frequency between the two ground-state phosphorus environments for (**5**) is similar to that in (**1**) and (**2**). The value of $\Delta G^{\ddagger}$ is very insensitive to this frequency parameter and the approximation gives an estimate for $\Delta G^{\ddagger}$ of *ca.* 35 kJ mol^{-1}. Thus, $\Delta G^{\ddagger}$ for the intramolecular metal core rearrangements of (**1**), (**2**), and (**5**) falls in descending order of Group 1B metal congeners.

Johnson[27] has very recently proposed that polyhedral rearrangements in cluster compounds occur *via* mechanisms which involve the cleavage of only one M–M contact at a time. Two mechanisms (labelled A and B in Figure 4) which minimize the breaking of M–M contacts are possible for the coinage metal site exchange in (**1**), (**2**), and (**5**). Mechanism B is very closely related to the restricted Berry pseudo-rotation that we have previously proposed[3] to explain similar skeletal rearrangements in the pentanuclear species $[Au_2Ru_3(\mu_3\text{-}S)(CO)_8L(PPh_3)_2]$ (L = CO or PPh_3). In addition, we have very recently reported[26] some indirect evidence to support mechanism B for the metal core rearrangements of (**1**), (**2**), and (**5**).

The ambient temperature $^{13}C\text{-}\{^1H\}$ n.m.r. spectra of (**1**), (**2**), and (**5**) all show a singlet CO peak, indicating that a further fluxional process involving complete CO group site exchange

Table 5. Selected bond lengths (Å) and angles (°), with estimated standard deviations in parentheses, for $[Au_2Ru_4(\mu_3\text{-}H)(\mu\text{-}H)(CO)_{12}(PPh_3)_2]$ (**5**)

Au(1)–Au(2)	2.791(1)	Au(1)–Ru(3)	2.844(1)	Ru(3)–C(7)	1.874(18)	Ru(3)–C(8)	1.897(16)
Au(1)–Ru(4)	2.840(1)	Au(1)–P(1)	2.294(4)	Ru(3)–C(9)	1.892(17)	Ru(4)–H(2)	1.847(103)
Au(2)–Ru(1)	3.091(1)	Au(2)–Ru(3)	2.859(1)	Ru(4)–C(10)	1.903(22)	Ru(4)–C(11)	1.928(16)
Au(2)–Ru(4)	2.949(1)	Au(2)–P(2)	2.275(4)	Ru(4)–C(12)	1.867(16)	P(1)–C(111)	1.856(18)
Au(2)–H(1)	2.038(105)	Ru(1)–Ru(2)	2.788(2)	P(1)–C(121)	1.782(15)	P(1)–C(131)	1.804(14)
Ru(1)–Ru(3)	2.966(2)	Ru(1)–Ru(4)	2.948(2)	P(2)–C(211)	1.824(17)	P(2)–C(221)	1.827(14)
Ru(1)–H(1)	1.762(75)	Ru(1)–H(2)	1.869(86)	P(2)–C(231)	1.805(14)	C(1)–O(1)	1.138(31)
Ru(1)–C(1)	1.923(23)	Ru(1)–C(2)	1.863(29)	C(2)–O(2)	1.177(39)	C(3)–O(3)	1.170(22)
Ru(1)–C(3)	1.850(17)	Ru(2)–Ru(3)	2.821(2)	C(4)–O(4)	1.117(22)	C(5)–O(5)	1.134(28)
Ru(2)–Ru(4)	2.817(2)	Ru(2)–C(4)	1.925(17)	C(6)–O(6)	1.150(19)	C(7)–O(7)	1.145(24)
Ru(2)–C(5)	1.898(23)	Ru(2)–C(6)	1.878(15)	C(8)–O(8)	1.150(21)	C(9)–O(9)	1.136(21)
Ru(3)–Ru(4)	3.011(2)	Ru(3)–H(1)	1.846(96)	C(10)–O(10)	1.127(27)	C(11)–O(11)	1.141(20)
				C(12)–O(12)	1.138(20)		

Au(2)–Au(1)–Ru(3)	61.0(1)	Au(2)–Au(1)–Ru(4)	63.2(1)	Ru(4)–Ru(3)–H(1)	77.6(31)	Au(1)–Ru(3)–C(7)	70.7(5)
Ru(3)–Au(1)–Ru(4)	64.0(1)	Au(2)–Au(1)–P(1)	134.6(1)	Au(2)–Ru(3)–C(7)	129.2(5)	Ru(1)–Ru(3)–C(7)	144.9(5)
Ru(3)–Au(1)–P(1)	146.8(1)	Ru(4)–Au(1)–P(1)	145.9(1)	Ru(2)–Ru(3)–C(7)	88.5(5)	Ru(4)–Ru(3)–C(7)	96.9(5)
Au(1)–Au(2)–Ru(1)	106.9(1)	Au(1)–Au(2)–Ru(3)	60.4(1)	H(1)–Ru(3)–C(7)	173.7(31)	Au(1)–Ru(3)–C(8)	78.7(5)
Ru(1)–Au(2)–Ru(3)	59.6(1)	Au(1)–Au(2)–Ru(4)	59.2(1)	Au(2)–Ru(3)–C(8)	72.0(5)	Ru(1)–Ru(3)–C(8)	118.9(6)
Ru(1)–Au(2)–Ru(4)	58.4(1)	Ru(3)–Au(2)–Ru(4)	62.4(1)	Ru(2)–Ru(3)–C(8)	173.1(6)	Ru(4)–Ru(3)–C(8)	126.9(5)
Au(1)–Au(2)–P(2)	123.6(1)	Ru(1)–Au(2)–P(2)	129.4(1)	H(1)–Ru(3)–C(8)	85.2(30)	C(7)–Ru(3)–C(8)	95.8(8)
Ru(3)–Au(2)–P(2)	145.2(1)	Ru(4)–Au(2)–P(2)	152.2(1)	Au(1)–Ru(3)–C(9)	159.5(6)	Au(2)–Ru(3)–C(9)	136.3(6)
Au(1)–Au(2)–H(1)	100.1(30)	Ru(1)–Au(2)–H(1)	32.7(18)	Ru(1)–Ru(3)–C(9)	91.5(6)	Ru(2)–Ru(3)–C(9)	81.8(5)
Ru(3)–Au(2)–H(1)	40.0(28)	Ru(4)–Au(2)–H(1)	76.7(33)	Ru(4)–Ru(3)–C(9)	138.0(5)	H(1)–Ru(3)–C(9)	94.2(34)
P(2)–Au(2)–H(1)	125.1(34)	Au(2)–Ru(1)–Ru(2)	104.0(1)	C(7)–Ru(3)–C(9)	92.0(8)	C(8)–Ru(3)–C(9)	92.6(7)
Au(2)–Ru(1)–Ru(3)	56.3(1)	Ru(2)–Ru(1)–Ru(3)	58.6(1)	Au(1)–Ru(4)–Au(2)	57.6(1)	Au(1)–Ru(4)–Ru(1)	109.6(1)
Au(2)–Ru(1)–Ru(4)	58.4(1)	Ru(2)–Ru(1)–Ru(4)	58.8(1)	Au(2)–Ru(4)–Ru(1)	63.2(1)	Au(1)–Ru(4)–Ru(2)	108.2(1)
Ru(3)–Ru(1)–Ru(4)	61.2(1)	Au(2)–Ru(1)–H(1)	38.6(33)	Au(2)–Ru(4)–Ru(2)	107.0(1)	Ru(1)–Ru(4)–Ru(2)	57.8(1)
Ru(2)–Ru(1)–H(1)	94.1(36)	Ru(3)–Ru(1)–H(1)	35.6(36)	Au(1)–Ru(4)–Ru(3)	58.1(1)	Au(2)–Ru(4)–Ru(3)	57.3(1)
Ru(4)–Ru(1)–H(1)	80.6(40)	Au(2)–Ru(1)–H(2)	61.8(31)	Ru(1)–Ru(4)–Ru(3)	59.7(1)	Ru(2)–Ru(4)–Ru(3)	57.8(1)
Ru(2)–Ru(1)–H(2)	89.5(31)	Ru(3)–Ru(1)–H(2)	94.3(32)	Au(1)–Ru(4)–H(2)	123.1(28)	Au(2)–Ru(4)–H(2)	65.5(28)
Ru(4)–Ru(1)–H(2)	37.2(32)	H(1)–Ru(1)–H(2)	98.6(48)	Ru(1)–Ru(4)–H(2)	37.8(27)	Ru(2)–Ru(4)–H(2)	89.1(32)
Au(2)–Ru(1)–C(1)	73.9(7)	Ru(2)–Ru(1)–C(1)	169.5(6)	Ru(3)–Ru(4)–H(2)	93.4(24)	Au(1)–Ru(4)–C(10)	68.6(5)
Ru(3)–Ru(1)–C(1)	124.8(6)	Ru(4)–Ru(1)–C(1)	112.9(7)	Au(2)–Ru(4)–C(10)	126.2(5)	Ru(1)–Ru(4)–C(10)	145.2(5)
H(1)–Ru(1)–C(1)	90.4(35)	H(2)–Ru(1)–C(1)	80.5(31)	Ru(2)–Ru(4)–C(10)	88.9(5)	Ru(3)–Ru(4)–C(10)	95.5(5)
Au(2)–Ru(1)–C(2)	126.1(8)	Ru(2)–Ru(1)–C(2)	90.0(10)	H(2)–Ru(4)–C(10)	168.1(29)	Au(1)–Ru(4)–C(11)	76.9(5)
Ru(3)–Ru(1)–C(2)	92.3(8)	Ru(4)–Ru(1)–C(2)	146.0(9)	Au(2)–Ru(4)–C(11)	72.1(5)	Ru(1)–Ru(4)–C(11)	117.2(6)
H(1)–Ru(1)–C(2)	89.5(37)	H(2)–Ru(1)–C(2)	171.9(35)	Ru(2)–Ru(4)–C(11)	173.6(5)	Ru(3)–Ru(4)–C(11)	124.4(4)
C(1)–Ru(1)–C(2)	99.5(12)	Au(2)–Ru(1)–C(3)	142.4(5)	H(2)–Ru(4)–C(11)	84.8(32)	C(10)–Ru(4)–C(11)	96.6(7)
Ru(2)–Ru(1)–C(3)	82.9(6)	Ru(3)–Ru(1)–C(3)	141.4(7)	Au(1)–Ru(4)–C(12)	157.7(6)	Au(2)–Ru(4)–C(12)	140.2(6)
Ru(4)–Ru(1)–C(3)	98.0(6)	H(1)–Ru(1)–C(3)	177.0(44)	Ru(1)–Ru(4)–C(12)	92.5(6)	Ru(2)–Ru(4)–C(12)	81.3(5)
H(2)–Ru(1)–C(3)	81.7(32)	C(1)–Ru(1)–C(3)	92.7(9)	Ru(3)–Ru(4)–C(12)	138.1(5)	H(2)–Ru(4)–C(12)	76.1(27)
C(2)–Ru(1)–C(3)	90.2(9)	Ru(1)–Ru(2)–Ru(3)	63.8(1)	C(10)–Ru(4)–C(12)	92.0(8)	C(11)–Ru(4)–C(12)	95.3(7)
Ru(1)–Ru(2)–Ru(4)	63.4(1)	Ru(3)–Ru(2)–Ru(4)	64.6(1)	Au(1)–P(1)–C(111)	115.9(5)	Au(1)–P(1)–C(121)	112.5(6)
Ru(1)–Ru(2)–C(4)	100.6(7)	Ru(3)–Ru(2)–C(4)	100.6(5)	C(111)–P(1)–C(121)	104.7(8)	Au(1)–P(1)–C(131)	112.5(5)
Ru(4)–Ru(2)–C(4)	161.4(6)	Ru(1)–Ru(2)–C(5)	157.3(5)	C(111)–P(1)–C(131)	103.9(7)	C(121)–P(1)–C(131)	106.4(7)
Ru(3)–Ru(2)–C(5)	97.1(5)	Ru(4)–Ru(2)–C(5)	98.1(5)	Au(2)–P(2)–C(211)	111.4(4)	Au(2)–P(2)–C(221)	114.9(5)
C(4)–Ru(2)–C(5)	94.8(8)	Ru(1)–Ru(2)–C(6)	101.7(6)	C(211)–P(2)–C(221)	103.8(7)	Au(2)–P(2)–C(231)	114.8(5)
Ru(3)–Ru(2)–C(6)	161.9(5)	Ru(4)–Ru(2)–C(6)	99.9(4)	C(211)–P(2)–C(231)	104.7(7)	C(221)–P(2)–C(231)	106.3(6)
C(4)–Ru(2)–C(6)	92.5(7)	C(5)–Ru(2)–C(6)	94.1(8)	Au(2)–H(1)–Ru(1)	108.7(38)	Au(2)–H(1)–Ru(3)	94.7(49)
Au(1)–Ru(3)–Au(2)	58.6(1)	Au(1)–Ru(3)–Ru(1)	109.0(1)	Ru(1)–H(1)–Ru(3)	110.6(59)	Ru(1)–H(2)–Ru(4)	105.0(49)
Au(2)–Ru(3)–Ru(1)	64.1(1)	Au(1)–Ru(3)–Ru(2)	108.0(1)	Ru(1)–C(1)–O(1)	170.2(17)	Ru(1)–C(2)–O(2)	177.9(25)
Au(2)–Ru(3)–Ru(2)	109.4(1)	Ru(1)–Ru(3)–Ru(2)	57.5(1)	Ru(1)–C(3)–O(3)	176.8(19)	Ru(2)–C(4)–O(4)	177.1(21)
Au(1)–Ru(3)–Ru(4)	57.9(1)	Au(2)–Ru(3)–Ru(4)	60.2(1)	Ru(2)–C(5)–O(5)	174.4(14)	Ru(2)–C(6)–O(6)	173.9(14)
Ru(1)–Ru(3)–Ru(4)	59.1(1)	Ru(2)–Ru(3)–Ru(4)	57.7(1)	Ru(3)–C(7)–O(7)	172.6(14)	Ru(3)–C(8)–O(8)	174.0(15)
Au(1)–Ru(3)–H(1)	103.4(34)	Au(2)–Ru(3)–H(1)	45.3(34)	Ru(3)–C(9)–O(9)	173.3(15)	Ru(4)–C(10)–O(10)	170.9(15)
Ru(1)–Ru(3)–H(1)	33.8(29)	Ru(2)–Ru(3)–H(1)	91.2(30)	Ru(4)–C(11)–O(11)	171.6(13)	Ru(4)–C(12)–O(12)	176.1(14)

occurs for these species. At −90 °C, it is possible to obtain a pattern of CO signals consistent with the ground-state structures for (**1**) and (**2**), but only two, very considerably broadened, peaks are visible for (**5**). Thus, $\Delta G^{\ddagger}$ for the CO group site exchange seems to be higher for the clusters containing the two lighter coinage metals.

Experimental

All reactions and manipulations were performed under an atmosphere of dry oxygen-free nitrogen, using Schlenk-tube techniques.[28] Solvents were freshly distilled under nitrogen from the usual drying agents immediately before use. Light petroleum refers to that fraction of b.p. 40—60 °C. Established methods were used to prepare the salt $[N(PPh_3)_2]_2[Ru_4(\mu\text{-}H)_2(CO)_{12}]$,[9] and the complexes $[Cu(NCMe)_4]PF_6$[29] and $[AgI(PPh_3)]$.[30] The compounds $[Ag(NCMe)_4]PF_6$,[29] $[CuCl(PPh_3)]$,[31] and $[AuCl(PPh_3)]$[32] were synthesized by adaptation of published routes. Analytical and other physical data for the new compounds are presented in Table 1, together with their i.r. spectra. Table 2 summarizes the results of n.m.r. spectroscopy measurements.

Infrared spectra were recorded on a Nicolet FT MX-1 spectrophotometer. Hydrogen-1 and $^{13}C\text{-}\{^1H\}$ n.m.r. spectra

Table 6. Crystal structure analyses of (**1**), (**2**), and (**5**)

Cluster	(**1**)·CH_2Cl_2	(**2**)·CH_2Cl_2	(**5**)·CH_2Cl_2
(*a*) Data collection[a]			
Crystal colour and habit	Red prism	Red prism	Red rod
Crystal size/mm	0.5 × 0.25 × 0.1	0.38 × 0.3 × 0.2	0.5 × 0.22 × 0.15
2θ range/°	4—50	4—50	4—45
Scan method	θ—2θ	θ—2θ	Wyckoff ω
Scan speed range/° min^{-1}	2—29.3	2—29.3	2.9—29.3
No. of azimuthal scan data	210	212	—
Transmission coefficient range	0.372—0.491	0.487—0.621	0.093—0.360
No. of data collected	8 543	7 528	7 928
No. of unique data	7 762	6 694	7 105
No. of 'observed' data (n.o.)	6 300	5 813	4 468
'Observed' criterion, n [$I > n\sigma(I)$]	2.5	2.5	3.0
(*b*) Structure solution and refinement[b]			
Anisotropic atoms	Cu, Ru, C, O. P, Cl	Ag, Ru, C, O, P	Au, Ru, C, O. P, Cl
Isotropic atoms	Disordered phenyl C, C of CH_2Cl_2, H	CH_2Cl_2, H	Phenyl C, H
No. of variables (n.v.)	543	633	462
R	0.042	0.047	0.047
R'	0.044	0.048	0.048
g	0.0007	0.0007	0.0009
S	1.32	1.52	1.16
Largest final difference electron density features/e $Å^{-3}$	1.00	1.3	1.9

[a] Data were collected at room temperature on Nicolet *P3m* diffractometers for unique portions of reciprocal space, using graphite-monochromated *X*-radiation. [b] Structures were solved by conventional Patterson and Fourier techniques and refined by blocked-cascade full-matrix least squares. $R = \Sigma||F_o| - |F_c||/\Sigma|F_o|$, $R' = \Sigma w^{\frac{1}{2}}||F_o| - |F_c||/\Sigma w^{\frac{1}{2}}|F_o|$, $S = [\Sigma w(|F_o| - |F_c|)^2/\Sigma(\text{n.o.} - \text{n.v.})]^{\frac{1}{2}}$.

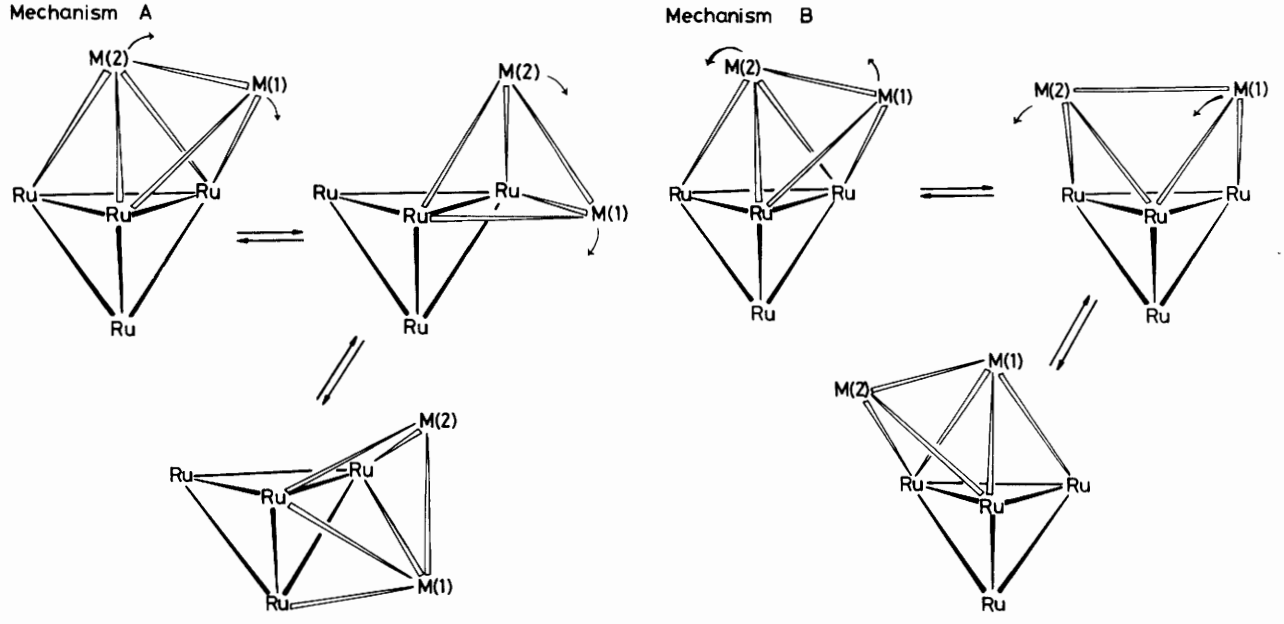

Figure 4. Two possible mechanisms for the coinage metal site exchange in (**1**), (**2**), and (**5**). Both mechanisms minimize the breaking of metal–metal contacts, as proposed by Johnson.[27] All of the ligands have been omitted for clarity, but both mechanisms must also involve a concomitant site-exchange process for the two hydrido ligands

were measured on a JEOL FX 200 spectrometer and ^{31}P-{^1H} n.m.r. spectra on a JEOL FX 90Q instrument. Product separation by column chromatography was performed on Aldrich Florisil (100—200 mesh) or B. D. H. alumina (Brockman activity II).

Synthesis of the Compounds $[M_2Ru_4(\mu_3\text{-}H)_2(CO)_{12}(PPh_3)_2]$ (M = Cu *or* Ag).—A dichloromethane (70 cm^3) solution of $[N(PPh_3)_2]_2[Ru_4(\mu\text{-}H)_2(CO)_{12}]$ (1.20 g, 0.66 mmol) at −30 °C was treated with a solution of $[Cu(NCMe)_4]PF_6$ (0.49 g, 1.32 mmol) in dichloromethane (50 cm^3) and then, after stirring the reaction mixture at −30 °C for 1 min, a dichloromethane (30 cm^3) solution of PPh_3 (0.35 g, 1.34 mmol) was added. The mixture was allowed to warm to ambient temperature with stirring and the solvent was then removed under reduced pressure. The crude residue was extracted with dichloro-

Table 7. Atomic positional parameters (fractional co-ordinates) ($\times 10^4$) for (1)·CH_2Cl_2, with estimated standard deviations in parentheses

Atom	*x*	*y*	*z*	Atom	*x*	*y*	*z*
Ru(2)	1 846(1)	2 345(1)	975(1)	C(132)	7 183(6)	2 396(5)	1 420(5)
Ru(4)	3 590(1)	3 062(1)	886(1)	C(133)	7 942	2 742	678
Ru(1)	1 457(1)	4 056(1)	1 648(1)	C(134)	8 613	2 118	106
Ru(3)	2 435(1)	2 125(1)	2 670(1)	C(135)	8 525	1 146	275
Cu(1)	4 497(1)	1 977(1)	2 322(1)	C(136)	7 765	800	1 017
Cu(2)	3 173(1)	3 714(1)	2 478(1)	C(131)	7 094	1 424	1 590
P(1)	6 065(2)	1 039(1)	2 565(1)	C(212)	3 440(7)	6 318(6)	1 728(6)
P(2)	3 490(1)	4 643(1)	3 268(1)	C(213)	3 526	7 277	1 286
C(5)	2 499(9)	1 141(8)	596(6)	C(214)	3 850	7 840	1 730
C(4)	579(8)	1 929(7)	1 549(6)	C(215)	4 086	7 444	2 616
C(6)	1 451(7)	2 921(7)	−183(6)	C(216)	3 999	6 486	3 058
C(10)	4 376(7)	1 878(5)	533(5)	C(211)	3 676	5 923	2 614
C(12)	3 462(6)	3 612(6)	−370(5)	C(262)	3 511(8)	6 078(6)	1 750(6)
C(11)	4 707(5)	3 658(5)	837(5)	C(263)	3 452	7 049	1 266
C(2)	83(6)	3 837(7)	2 090(6)	C(264)	3 207	7 798	1 761
C(3)	1 207(6)	4 736(6)	455(6)	C(265)	3 022	7 577	2 741
C(1)	1 194(6)	5 235(6)	2 131(6)	C(266)	3 081	6 607	3 225
C(7)	3 028(7)	859(6)	2 409(5)	C(261)	3 326	5 857	2 729
C(8)	2 939(6)	1 993(5)	3 765(5)	C(222)	5 553(7)	4 879(6)	2 952(6)
C(9)	1 184(7)	1 737(8)	3 368(6)	C(223)	6 563	4 661	3 105
O(5)	2 855(8)	406(5)	378(5)	C(224)	6 871	3 865	3 801
O(4)	−154(6)	1 640(7)	1 890(5)	C(225)	6 168	3 287	4 345
O(6)	1 189(7)	3 239(6)	−889(5)	C(226)	5 158	3 505	4 192
O(10)	4 875(5)	1 204(4)	263(4)	C(221)	4 850	4 301	3 496
O(12)	3 438(5)	3 947(5)	−1 148(4)	C(232)	3 058(6)	4 709(7)	5 212(6)
O(11)	5 366(4)	4 044(4)	699(4)	C(233)	2 415	4 672	6 105
O(2)	−748(4)	3 752(7)	2 372(5)	C(234)	1 441	4 445	6 278
O(3)	1 093(5)	5 188(5)	−277(4)	C(235)	1 109	4 255	5 558
O(1)	948(5)	5 960(5)	2 347(5)	C(236)	1 751	4 293	4 665
O(7)	3 362(7)	80(4)	2 331(4)	C(231)	2 725	4 520	4 491
O(8)	3 140(5)	1 833(4)	4 491(4)	C(242)	1 849(8)	5 937(6)	4 292(7)
O(9)	450(6)	1 501(8)	3 814(5)	C(243)	1 011	6 107	5 040
C(111)	6 213(6)	−253(5)	2 603(5)	C(244)	691	5 320	5 713
C(112)	5 883(10)	−523(6)	1 949(6)	C(245)	1 209	4 362	5 638
C(113)	5 981(13)	−1 500(7)	1 959(7)	C(246)	2 046	4 192	4 890
C(114)	6 443(11)	−2 201(7)	2 615(7)	C(241)	2 366	4 979	4 217
C(115)	6 756(9)	−1 954(6)	3 274(7)	C(252)	4 587(7)	3 900(8)	4 677(6)
C(116)	6 659(7)	−980(5)	3 258(5)	C(253)	5 504	3 455	5 002
C(121)	6 521(5)	1 013(5)	3 610(5)	C(254)	6 449	3 275	4 364
C(122)	5 823(6)	943(5)	4 467(5)	C(255)	6 476	3 540	3 401
C(123)	6 156(7)	820(6)	5 292(6)	C(256)	5 559	3 985	3 076
C(124)	7 184(7)	758(6)	5 264(6)	C(251)	4 614	4 165	3 714
C(125)	7 881(7)	827(7)	4 412(7)	C	−385(18)	8 209(17)	3 787(18)
C(126)	7 564(6)	952(6)	3 578(6)	Cl(1)	−229(9)	8 715(11)	2 405(10)
				Cl(2)	809(12)	8 857(11)	3 295(14)

methane–diethyl ether (1:4; 50 cm^3 portions) until the extracts were no longer coloured red and the combined extracts were then filtered through a Celite pad (*ca.* 1 × 3 cm). After removal of the solvent under reduced pressure, the residue was dissolved in dichloromethane–light petroleum (1:1) and chromatographed at −20 °C on a Florisil column (20 × 3 cm). Elution with dichloromethane–light petroleum (1:1) afforded one dark red fraction, which, after removal of the solvent under reduced pressure and crystallization of the residue from dichloromethane–light petroleum, yielded dark red *microcrystals* of $[Cu_2Ru_4(\mu_3\text{-}H)_2(CO)_{12}(PPh_3)_2]$ (**1**) (0.70 g).

Dark red *microcrystals* of $[Ag_2Ru_4(\mu_3\text{-}H)_2(CO)_{12}(PPh_3)_2]$ (**2**) (0.72 g) were synthesized by the same procedure, using $[Ag(NCMe)_4]PF_6$ (0.55 g, 1.32 mmol) in place of $[Cu(NCMe)_4]PF_6$. The chromatography was performed on an alumina column (20 × 3 cm) at −20 °C.

Alternatively, compounds (**1**) (0.29 g, 50%) and (**2**) (0.32 g, 52%) can also be synthesized, in reduced yield, by the route described below for the gold–ruthenium cluster (**5**). The complexes $[CuCl(PPh_3)]$ (0.31 g, 0.86 mmol) and $[AgI(PPh_3)]$ (0.42 g, 0.85 mmol) were utilized for (**1**) and (**2**), respectively, instead of $[AuCl(PPh_3)]$ and the conditions for chromatography and crystallization were the same as those described above.

Synthesis of the Compound $[Au_2Ru_4(\mu_3\text{-}H)(\mu\text{-}H)(CO)_{12}(PPh_3)_2]$.—An acetone (50 cm^3) solution of $[N(PPh_3)_2]_2[Ru_4(\mu\text{-}H)_2(CO)_{12}]$ (0.76 g, 0.42 mmol) was treated with a dichloromethane (30 cm^3) solution of $[AuCl(PPh_3)]$ (0.42 g, 0.85 mmol) and solid $TlPF_6$ (0.50 g, 1.43 mmol) and the mixture was stirred at room temperature for 0.25 h. After filtration of the dark red mixture through a Celite pad (*ca.* 1 × 3 cm), the solvent was removed under reduced pressure and the crude residue was dissolved in dichloromethane–light petroleum (1:2). Chromatography on an alumina column (20 × 3 cm), eluting with dichloromethane–light petroleum (1:2), afforded a dark red fraction containing the product, followed by a small dark green fraction containing $[Au_3Ru_4(\mu_3\text{-}H)(CO)_{12}(PPh_3)_3]$ (0.05 g, 6%). After removal of the solvent from the first fraction under reduced pressure, crystallization of the residue from

Table 8. Atomic positional parameters (fractional co-ordinates) ($\times 10^4$) for (**2**)·CH_2Cl_2, with estimated standard deviations in parentheses

Atom	*x*	*y*	*z*	Atom	*x*	*y*	*z*
Ag(1)	4 544(1)	1 928(1)	2 270(1)	C(116)	6 767(8)	−1 026(7)	3 252(7)
Ag(2)	3 232(1)	3 765(1)	2 410(1)	C(121)	6 595(7)	946(6)	3 569(6)
Ru(1)	1 456(1)	4 050(1)	1 569(1)	C(122)	7 605(7)	872(7)	3 563(7)
Ru(2)	1 791(1)	2 392(1)	941(1)	C(123)	7 876(9)	733(8)	4 418(9)
Ru(3)	3 554(1)	3 044(1)	756(1)	C(124)	7 169(10)	680(7)	5 272(8)
Ru(4)	2 385(1)	2 116(1)	2 636(1)	C(125)	6 166(10)	765(8)	5 277(8)
P(1)	6 200(2)	961(2)	2 527(2)	C(126)	5 889(8)	876(7)	4 428(7)
P(2)	3 618(2)	4 641(2)	3 293(2)	C(131)	7 218(8)	1 362(8)	1 507(7)
C(1)	1 231(8)	5 180(7)	2 033(8)	C(132)	7 949(10)	747(10)	1 007(9)
C(2)	1 196(7)	4 769(7)	376(8)	C(133)	8 673(11)	1 133(11)	243(9)
C(3)	108(7)	3 858(8)	2 085(7)	C(134)	8 703(12)	2 037(16)	−2(11)
C(4)	1 402(9)	2 992(8)	−240(7)	C(135)	7 988(10)	2 657(11)	520(10)
C(5)	2 406(9)	1 206(8)	606(7)	C(136)	7 253(10)	2 322(9)	1 206(10)
C(6)	538(10)	2 007(9)	1 515(8)	C(211)	4 905(8)	4 161(7)	3 502(7)
C(7)	4 311(7)	1 868(6)	461(6)	C(212)	5 732(9)	4 318(11)	2 748(10)
C(8)	4 696(7)	3 605(7)	594(7)	C(213)	6 720(12)	3 908(12)	2 801(14)
C(9)	3 391(8)	3 556(7)	−507(7)	C(214)	6 923(12)	3 377(12)	3 643(12)
C(10)	3 030(8)	891(7)	2 398(6)	C(215)	6 169(10)	3 174(8)	4 374(11)
C(11)	2 791(7)	1 978(7)	3 772(6)	C(216)	5 167(10)	3 511(8)	4 303(9)
C(12)	1 168(9)	1 688(9)	3 305(8)	C(221)	2 756(9)	4 593(7)	4 479(7)
O(1)	988(7)	5 874(6)	2 285(7)	C(222)	3 034(11)	4 754(8)	5 214(8)
O(2)	1 103(6)	5 223(6)	−363(6)	C(223)	2 356(14)	4 667(10)	6 137(9)
O(3)	−718(6)	3 796(7)	2 383(6)	C(224)	1 393(12)	4 453(12)	6 226(13)
O(4)	1 161(8)	3 315(7)	−953(6)	C(225)	1 188(11)	4 270(11)	5 534(11)
O(5)	2 719(8)	484(6)	404(6)	C(226)	1 877(8)	4 316(8)	4 688(9)
O(6)	−227(7)	1 788(8)	1 876(7)	C(231)	3 631(8)	5 898(7)	2 727(7)
O(7)	4 785(6)	1 190(5)	224(5)	C(232)	3 900(13)	6 469(9)	3 159(10)
O(8)	5 389(5)	3 948(5)	380(6)	C(233)	3 908(16)	7 430(11)	2 695(11)
O(9)	3 351(6)	3 838(6)	−1 283(5)	C(234)	3 624(11)	7 804(8)	1 863(9)
O(10)	3 384(6)	127(5)	2 306(5)	C(235)	3 421(9)	7 279(8)	1 415(9)
O(11)	2 938(7)	1 826(6)	4 515(5)	C(236)	3 419(8)	6 318(8)	1 852(8)
O(12)	440(7)	1 427(7)	3 749(6)	Cl(1)	884(31)	7 291(31)	4 425(31)
C(111)	6 336(7)	−307(7)	2 589(6)	C	27(29)	8 108(29)	3 728(27)
C(112)	5 980(9)	−553(8)	1 945(7)	Cl(3)	−200(25)	8 392(24)	2 633(24)
C(113)	6 068(11)	−1 484(8)	1 972(8)	Cl(4)	544(28)	9 000(26)	2 626(26)
C(114)	6 517(10)	−2 204(8)	2 634(8)	Cl(5)	845(25)	8 894(24)	3 540(27)
C(115)	6 822(11)	−1 979(8)	3 296(8)				

dichloromethane–light petroleum yielded dark red *microcrystals* of $[Au_2Ru_4(\mu_3\text{-}H)(\mu\text{-}H)(CO)_{12}(PPh_3)_2]$ (**5**) (0.42 g).

Crystal Structure Determinations for (**1**)·CH_2Cl_2, (**2**)·CH_2Cl_2, *and* (**5**)·CH_2Cl_2.—Suitable crystals of (**1**)·CH_2Cl_2 and (**2**)·CH_2Cl_2 were grown from dichloromethane–light petroleum by slow layer diffusion at −20 °C. Crystals of (**5**)·CH_2Cl_2 were obtained from dichloromethane–diethyl ether–light petroleum, using the same technique.

Crystal data: for (**1**)·CH_2Cl_2. $C_{48}H_{32}Cu_2O_{12}P_2Ru_4$·$CH_2Cl_2$, M = 1 479.0, triclinic, space group $P\bar{1}$ (no. 2), a = 13.634(4), b = 14.485(5), c = 15.084(7) Å, α = 74.78(2), β = 74.59(2), γ = 74.37(2)°, U = 2 706(1) Å^3, Z = 2, D_c = 1.81 g cm^{-3}, $F(000)$ = 1 444, $\bar{\lambda}$ = 0.710 69 Å, μ(Mo-K_α) = 20.6 cm^{-1}.

For (**2**)·CH_2Cl_2. $C_{48}H_{32}Ag_2O_{12}P_2Ru_4$·$CH_2Cl_2$, M = 1 567.6, triclinic, space group $P\bar{1}$ (no. 2), a = 13.954(4), b = 14.928(3), c = 15.103(3) Å, α = 72.21(2), β = 72.64(2), γ = 73.36(2)°, U = 2 792(1) Å^3, Z = 2, D_c = 1.86 g cm^{-3}, $F(000)$ = 1 516, $\bar{\lambda}$ = 0.710 69 Å, μ(Mo-K_α) = 19.2 cm^{-1}.

For (**5**)·CH_2Cl_2. $C_{48}H_{32}Au_2O_{12}P_2Ru_4$·$CH_2Cl_2$, M = 1 745.8, monoclinic, space group $I2/a$ (non-standard setting of no. 15), a = 23.494(5), b = 13.334(3), c = 36.220(7) Å, β = 103.50(2)°, U = 11 032(4) Å^3, Z = 8, D_c = 2.10 g cm^{-3}, $F(000)$ = 6 239, $\bar{\lambda}$ = 0.710 69 Å, μ(Mo-K_α) = 64.5 cm^{-1}; crystal faces [distance from origin (mm)] (100) [0.08], ($\bar{1}$00) [0.08], (001) [0.11], (00$\bar{1}$) [0.11], (1$\bar{1}$0) [0.25], (11$\bar{1}$) [0.15].

Table 6 lists important details of the structure determinations of (**1**)·CH_2Cl_2, (**2**)·CH_2Cl_2, and (**5**)·CH_2Cl_2. In each case, crystals were sealed, under N_2, in thin-walled glass capillaries for *X*-ray measurements. Absorption corrections were applied, based on azimuthal scan data for (**1**)·CH_2Cl_2 and (**2**)·CH_2Cl_2 and by Gaussian quadrature, based on measured crystal shape, for (**5**)·CH_2Cl_2. Refinement was by blocked-cascade full-matrix least squares, with data assigned weights, $w = [\sigma_c^2(F_o) + gF_o^2]^{-1}$ where $\sigma_c^2(F_o)$ is based on counting statistics alone and g was chosen to give minimum variation of $\Sigma w(|F_o| - F_c|)^2$ as a function of $|F_o|$. Complex neutral-atom scattering factors were taken from ref. 33 and all calculations were carried out with the programs of the SHELXTL package[34] on a Nicolet *R3m/E* system. Final positional parameters for refined atoms are given in Tables 7, 8, and 9 for (**1**)·CH_2Cl_2, (**2**)·CH_2Cl_2, and (**5**)·CH_2Cl_2, respectively. For (**1**) and (**2**), the μ_3-H atoms were constrained to have Ru–H distances close to 1.80 Å and the two coinage metal M–H distances constrained to be near a common value which refined to Cu–H 1.62(5) Å in (**1**) and Ag–H 1.72(5) Å in (**2**). For all three structures, initial hydrido ligand positions were calculated indirectly.[10] These calculations indicate rather different sites for the μ_3-H ligands in (**5**) as compared with (**1**), with much longer Au···H distances. Therefore no constraints were placed on the Au···H distance, while the Ru···H distances were forced to be close to a common value [which refined to 1.83(6) Å].

In each structure, the dichloromethane showed signs of disorder, but only for (**2**)·CH_2Cl_2 was it possible to assign pairs

Table 9. Atomic positional parameters (fractional co-ordinates) ($\times 10^4$) for (**5**)·CH_2Cl_2, with estimated standard deviations in parentheses

Atom	*x*	*y*	*z*	Atom	*x*	*y*	*z*
Au(1)	494(1)	1 876(1)	1 584(1)	C(116)	−475(9)	2 504(12)	2 469(5)
Au(2)	1 305(1)	1 888(1)	1 131(1)	C(121)	−94(7)	4 179(11)	1 656(4)
Ru(1)	1 352(1)	−267(1)	825(1)	C(122)	−487(8)	4 863(12)	1 762(5)
Ru(2)	604(1)	−1 351(1)	1 171(1)	C(123)	−663(9)	5 749(14)	1 540(5)
Ru(3)	1 250(1)	200(1)	1 608(1)	C(124)	−460(10)	5 909(15)	1 231(6)
Ru(4)	252(1)	613(1)	935(1)	C(125)	−79(9)	5 224(13)	1 113(6)
P(1)	131(2)	3 070(3)	1 924(1)	C(126)	111(7)	4 359(11)	1 338(4)
P(2)	1 832(2)	3 264(3)	1 044(1)	C(131)	661(7)	3 456(10)	2 346(4)
C(1)	1 738(10)	569(17)	527(5)	C(132)	655(8)	4 413(12)	2 506(5)
O(1)	1 919(10)	994(14)	307(5)	C(133)	1 090(9)	4 645(14)	2 844(5)
C(2)	1 942(13)	−1 205(22)	998(7)	C(134)	1 482(9)	3 950(13)	3 006(5)
O(2)	2 323(11)	−1 788(20)	1 098(5)	C(135)	1 484(9)	3 023(13)	2 863(5)
C(3)	1 033(8)	−1 084(12)	416(5)	C(136)	1 077(8)	2 770(12)	2 531(5)
O(3)	858(8)	−1 605(9)	155(4)	C(211)	2 470(7)	2 920(10)	867(4)
C(4)	1 088(9)	−2 490(12)	1 359(5)	C(212)	2 821(9)	2 123(13)	1 045(6)
O(4)	1 350(8)	−3 170(9)	1 471(4)	C(213)	3 306(10)	1 804(16)	905(6)
C(5)	71(10)	−1 575(12)	1 485(4)	C(214)	3 432(11)	2 265(15)	629(6)
O(5)	−264(7)	−1 773(10)	1 653(4)	C(215)	3 106(12)	3 007(17)	448(7)
C(6)	161(8)	−2 081(11)	760(5)	C(216)	2 636(11)	3 389(16)	571(6)
O(6)	−84(7)	−2 602(10)	523(3)	C(221)	2 140(7)	3 977(10)	1 476(4)
C(7)	796(7)	18(11)	1 965(4)	C(222)	2 650(8)	4 479(11)	1 526(5)
O(7)	574(7)	−98(9)	2 212(4)	C(223)	2 861(10)	5 056(14)	1 856(5)
C(8)	1 767(8)	1 155(12)	1 897(5)	C(224)	2 540(10)	5 124(15)	2 113(6)
O(8)	2 098(6)	1 667(10)	2 094(4)	C(225)	2 011(10)	4 651(14)	2 068(6)
C(9)	1 746(8)	−885(12)	1 809(5)	C(226)	1 816(8)	4 047(12)	1 745(5)
O(9)	2 060(6)	−1 482(9)	1 960(3)	C(231)	1 440(7)	4 155(10)	703(4)
C(10)	−345(9)	521(12)	1 209(5)	C(232)	1 078(8)	3 810(12)	377(5)
O(10)	−747(7)	435(10)	1 327(4)	C(233)	777(10)	4 506(14)	105(6)
C(11)	44(7)	1 926(12)	724(4)	C(234)	852(9)	5 519(14)	167(6)
O(11)	−132(6)	2 644(9)	567(4)	C(235)	1 197(9)	5 838(14)	497(5)
C(12)	−198(9)	−88(12)	523(5)	C(236)	1 499(8)	5 178(13)	763(6)
O(12)	−490(7)	−466(9)	265(4)	C	2 922(47)	7 132(63)	376(25)
C(111)	−515(7)	2 691(10)	2 104(4)	Cl(1)	3 279(14)	8 267(32)	535(10)
C(112)	−1 051(8)	2 588(12)	1 833(5)	Cl(2)	3 268(13)	6 131(22)	703(10)
C(113)	−1 530(10)	2 324(14)	1 970(6)				
C(114)	−1 491(10)	2 161(14)	2 329(6)				
C(115)	−983(11)	2 203(16)	2 593(7)				

of separate sites for the chlorine atoms. In the other cases, the disorder was modelled by use of anisotropic displacement parameters. For (**1**), one of the PPh_3 ligands [that attached to Cu(2)] showed disorder of its phenyl rings, such that each ring adopted two orientations with occupancies 0.511(3) and 0.489(3), respectively [the major occupancy being for rings C(21*n*), C(22*n*), and C(23*n*)]. The disordered rings were constrained to D_{6h} symmetry with C–C = 1.395 Å. In all of the structures the molecules are separated by normal van der Waals contact distances.

Acknowledgements

One of us (I. D. S.) gratefully acknowledges the support and guidance given to him by Professor F. G. A. Stone, F.R.S., during some of the experiments described herein. In addition, we thank Mr. S. S. D. Brown for providing a crystal of $[Au_2Ru_4(\mu_3\text{-}H)(\mu\text{-}H)(CO)_{12}(PPh_3)_2]$ suitable for single-crystal *X*-ray diffraction studies, the Nuffield Foundation for partial support of the work, Johnson Matthey Ltd. for a generous loan of gold, silver, and ruthenium salts, and Mrs. L. J. Salter for drawing the diagrams.

References

1 Part 1, R. A. Brice, S. C. Pearse, I. D. Salter, and K. Henrick, *J. Chem. Soc., Dalton Trans.*, 1986, 2181.
2 For example, K. P. Hall and D. M. P. Mingos, *Prog. Inorg. Chem.*, 1984, **32**, 237; P. Braunstein and J. Rose, *Gold Bull.*, 1985, **18**, 17; P. G. Jones, *ibid.*, 1983, **16**, 114 and refs. therein.
3 L. J. Farrugia, M. J. Freeman, M. Green, A. G. Orpen, F. G. A. Stone, and I. D. Salter, *J. Organomet. Chem.*, 1983, **249**, 273.
4 L. W. Bateman, M. Green, K. A. Mead, R. M. Mills, I. D. Salter, F. G. A. Stone, and P. Woodward, *J. Chem. Soc., Dalton Trans.*, 1983, 2599.
5 J. A. K. Howard, I. D. Salter, and F. G. A. Stone, *Polyhedron*, 1984, **3**, 567.
6 M. J. Freeman, M. Green, A. G. Orpen, I. D. Salter, and F. G. A. Stone, *J. Chem. Soc., Chem. Commun.*, 1983, 1332.
7 S. S. D. Brown, I. D. Salter, and B. M. Smith, *J. Chem. Soc., Chem. Commun.*, 1985, 1439.
8 M. I. Bruce and B. K. Nicholson, *J. Organomet. Chem.*, 1983, **252**, 243.
9 K. E. Inkrott and S. G. Shore, *Inorg. Chem.*, 1979, **18**, 2817.
10 A. G. Orpen, *J. Chem. Soc., Dalton Trans.*, 1980, 2509.
11 W. B. Pearson, 'Lattice Spacings and Structures of Metals and Alloys,' Pergamon Press, London, 1951.
12 R. W. G. Wyckoff, 'Crystal Structures,' 2nd edn., Wiley Interscience, New York, 1963, vol. 1.
13 C. E. Briant, D. I. Gilmour, and D. M. P. Mingos, *J. Organomet. Chem.*, 1984, **267**, C52.
14 C. E. Briant, R. G. Smith, and D. M. P. Mingos, *J. Chem. Soc., Chem. Commun.*, 1984, 586.
15 B. K. Teo and K. Keating, *J. Am. Chem. Soc.*, 1984, **106**, 2224.
16 J. S. Bradley, R. L. Pruett, E. Hill, G. B. Ansell, M. E. Leonowicz, and M. A. Modrick, *Organometallics*, 1982, **1**, 748.
17 M. R. Churchill, S. A. Bezman, J. A. Osborn, and J. Wormald, *Inorg. Chem.*, 1972, **11**, 1818; D. M. Ho and R. Bau, *Inorg. Chim. Acta*, 1984, **84**, 213.
18 B. F. G. Johnson, D. A. Kaner, J. Lewis, P. R. Raithby, and M. J. Taylor, *Polyhedron*, 1982, **1**, 105.
19 E. Roland, K. Fischer, and H. Vahrenkamp, *Angew. Chem., Int. Ed. Engl.*, 1983, **22**, 326.

20 M. I. Bruce, O. bin Shawkataly, and B. K. Nicholson, *J. Organomet. Chem.*, 1985, **286**, 427.
21 M. I. Bruce, E. Horn, O. bin Shawkataly, and M. R. Snow, *J. Organomet. Chem.*, 1985, **280**, 289.
22 M. I. Bruce and B. K. Nicholson, *Organometallics*, 1984, **3**, 101.
23 S. R. Bunkhall, H. D. Holden, B. F. G. Johnson, J. Lewis, G. N. Pain, P. R. Raithby, and M. J. Taylor, *J. Chem. Soc., Chem. Commun.*, 1984, 25.
24 G. V. Goeden and K. G. Caulton, *J. Am. Chem. Soc.*, 1981, **103**, 7354.
25 S. S. D. Brown, I. J. Colquhoun, W. McFarlane, M. Murray, I. D. Salter, and V. Šik, *J. Chem. Soc., Chem. Commun.*, 1986, 53.
26 P. A. Bates, S. S. D. Brown, A. J. Dent, M. B. Hursthouse, G. F. M. Kitchen, A. G. Orpen, I. D. Salter, and V. Šik, *J. Chem. Soc., Chem. Commun.*, 1986, 600.
27 B. F. G. Johnson, *J. Chem. Soc., Chem. Commun.*, 1986, 27.
28 D. F. Shriver, 'The Manipulation of Air-Sensitive Compounds,' McGraw-Hill, New York, 1969.
29 G. J. Kubas, *Inorg. Synth.*, 1979, **19**, 90.
30 B-K. Teo and J. C. Calabrese, *Inorg. Chem.*, 1976, **15**, 2474.
31 G. B. Kauffman and L. A. Teter, *Inorg. Synth.*, 1963, **7**, 9.
32 F. G. Mann, A. F. Wells, and D. Purdie, *J. Chem. Soc.*, 1937, 1828.
33 'International Tables for *X*-Ray Crystallography,' Kynoch Press, Birmingham, 1975, vol. 4.
34 G. M. Sheldrick, SHELXTL programs for use with the Nicolet *X*-ray system, Cambridge 1976, updated Göttingen, 1981.

Received 12*th March* 1986; *Paper* 6/497